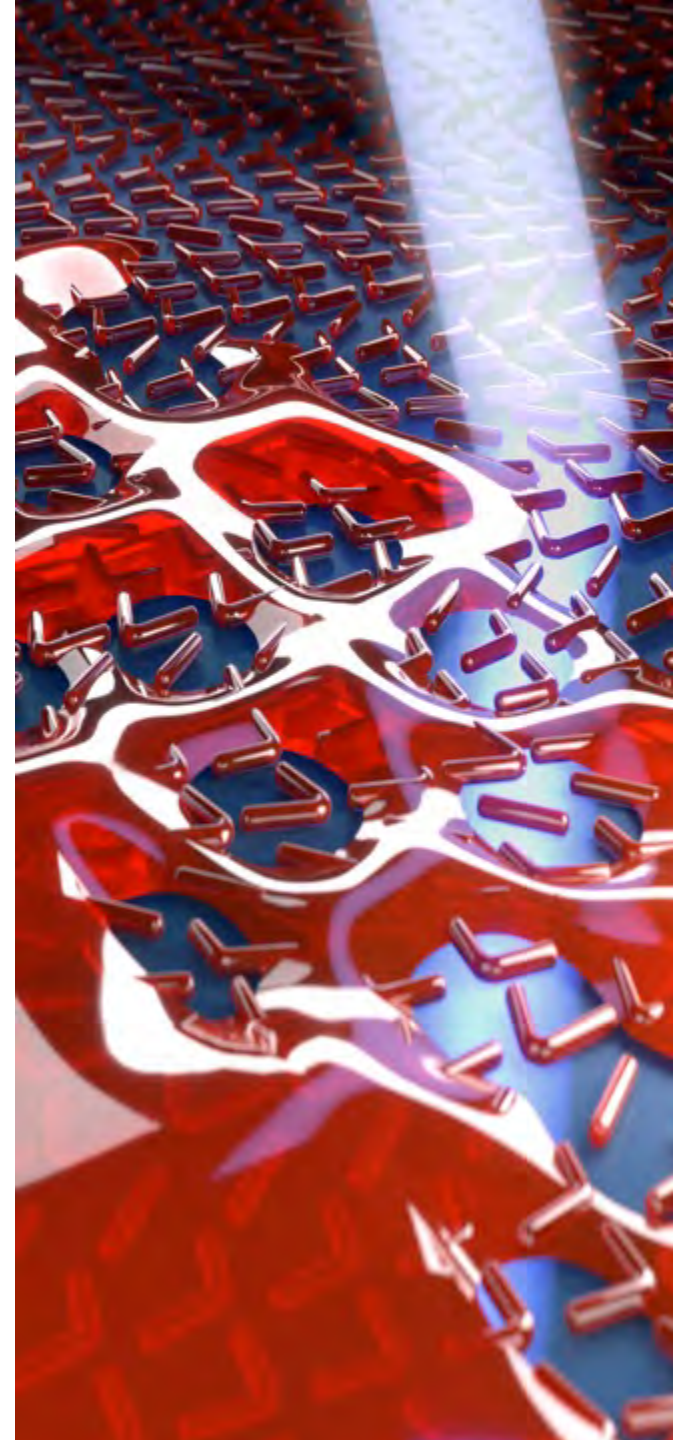


Structuration de Surface de Verres (de Chalcogenure)

Fabien Sorin

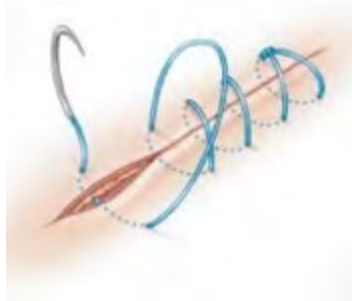
Associate Professor
Photonic Materials and Fiber Devices (FIMAP)
Institute of Materials (IMX)

The EPFL logo is centered at the bottom of the slide. It features the letters "EPFL" in a bold, red, sans-serif font. The "E" and "P" are connected, and the "F" and "L" are also connected.

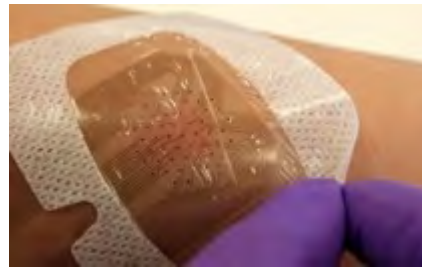
Health and personalized care



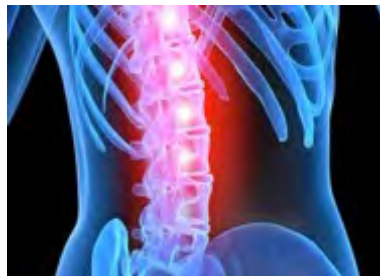
Bed sore prevention



Smart Sutures

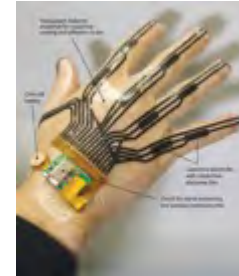


Wound dressing



Fiber probes, imaging, implants

Robotics, artificial skin and prosthetics



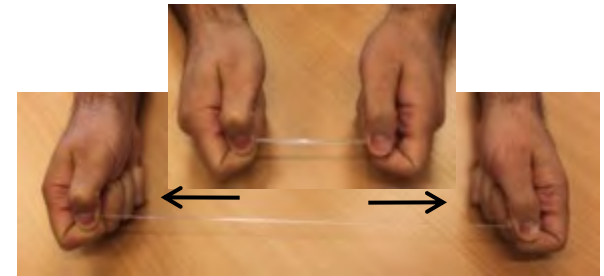
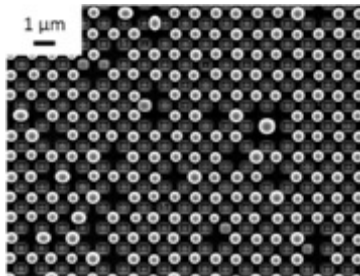
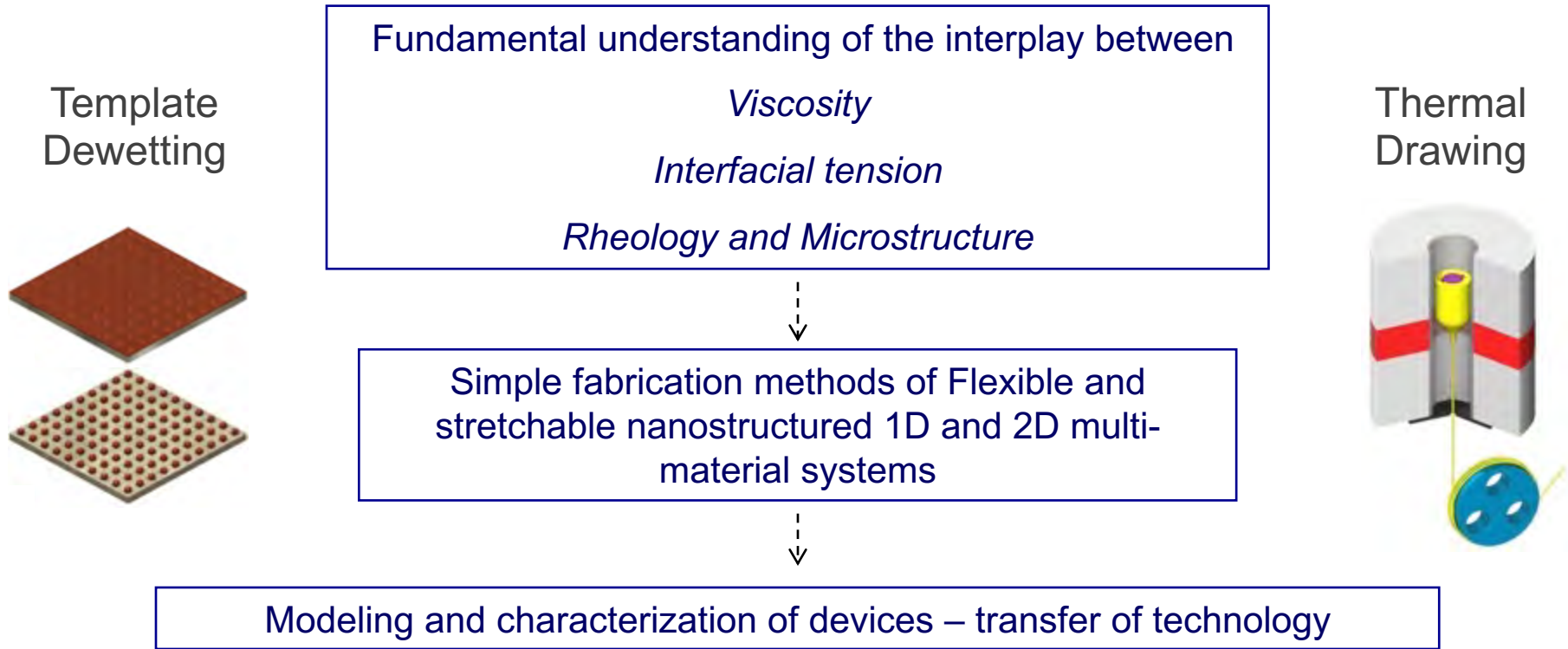
Smart cables and textiles

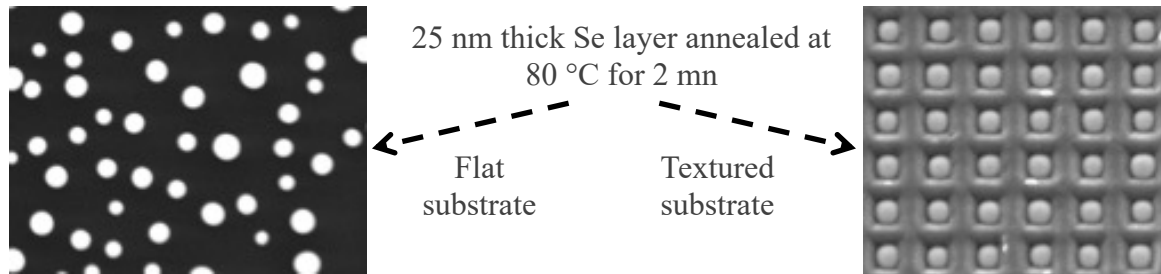


Sensing, Photonics, Energy



Engineering **fluid flow and instabilities** for the *scalable nano-fabrication* of **soft electronic and photonic devices** over large-area substrates, fibers and fabrics





- Dewetting of thin metal and polymeric films is a well-known phenomena, often unwanted
- An intriguing way to make optical nanostructures

Tableau périodique des éléments
et quelques-unes de leurs applications pratiques

remplissage des électrons au niveau s
remplissage des électrons au niveau p
remplissage des électrons au niveau d
remplissage des électrons au niveau f

1	2											18	18	18	10	8	2	
H	He											Ne	Ar	Kr	Xe	Rn		
3	4											13	14	15	16	17	18	
Li	Be											Al	Si	P	S	Cl	Ar	
11	12											31	32	33	34	35	36	
Na	Mg											Ga	Ge	As	Se	Br	Kr	
19	20											49	50	51	52	53	54	
K	Ca											In	Sn	Sb	Te	I	Xe	
37	38											81	82	83	84	85	86	
Rb	Sr											Tl	Pb	Bi	Po	At	Rn	
55	56											113	114	115	116	117	118	
Cs	Ba											Pb	Bi	Po	At	Rn		
87	88											201	202	203	204	205	206	
Fr	Ra											Tl	Pb	Bi	Po	At	Rn	
89	90											113	114	115	116	117	118	
La	Ce	Pr	Nd	Pm	Sm	Eu	Gd	Tb	Dy	Ho	Er	Tm	Yb					
57	58	59	60	61	62	63	64	65	66	67	68	69	70					
Ac	Th	Pa	U	Np	Pu	Am	Cm	Bk	Cf	Es	Fm	Md	No					
89	90	91	92	93	94	95	96	97	98	99	100	101	102					

Chalcogenide glasses combine:

- Optical properties:
 - Large index of refraction
 - Low attenuation in the visible
 - High non-linear properties
- Processing attributes
 - Resistant to crystallization
 - High viscosity
 - High surface energy

- Dewetting of thin Chalcogenide glasses films on topographically engineered substrates can be exploited to make advanced soft optical metasurfaces.

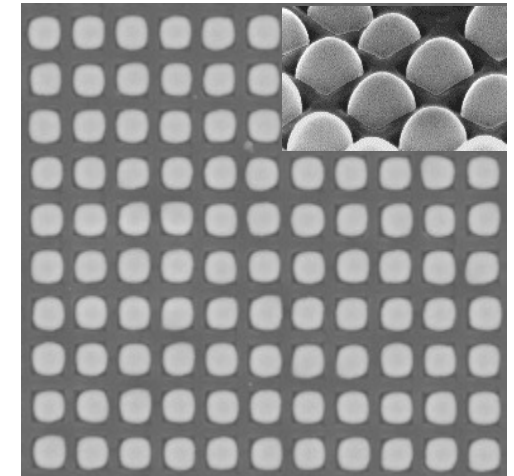
I. Reflow of Glass Surface Textures

- Fluid dynamic basic principles
- Reflow of a square shaped texture
- Reflow and thermal drawing



II. Reflow of a Glass Thin Film

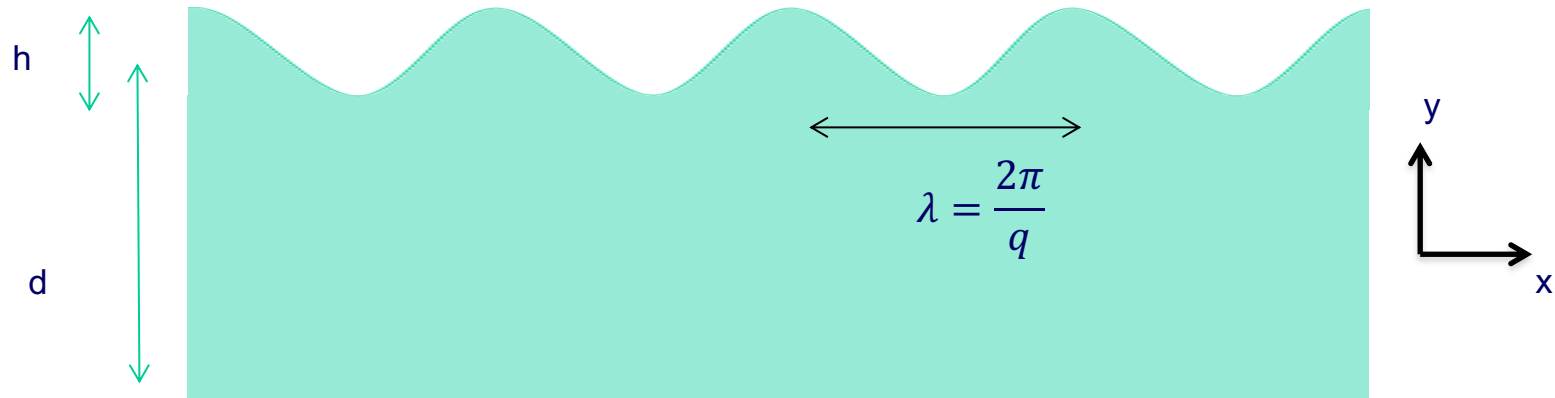
- Considering only reflow
- Dewetting and thermal drawing
- Examples of applications



III. Dewetting of a Glass thin film

- Taking into account disjoining pressure
- Templated dewetting of thin glasses
- Non-linear modelling

- We consider the following problem of the reflow of a surface roughness when a glass or a polymer is heated above its glass transition temperature and behaves like a viscous fluid.
- These types of issues arise in many areas in materials and glass science: lithography, optics, surface science etc...



- Surface tension: Laplace pressure

$$p = \gamma \kappa$$

- $y^s(x) = d + h \sin\left(\frac{2\pi}{\lambda} x\right)$

- $h, \lambda \ll d$, $hq \ll 1$

$$\kappa = \frac{\partial^2 h / \partial x^2}{\left(1 + \left(\frac{\partial h}{\partial x}\right)^2\right)^{3/2}}$$

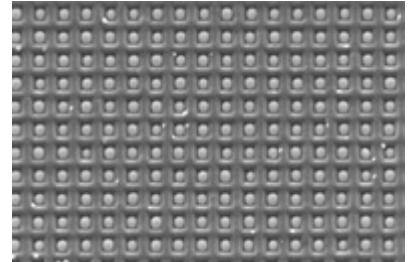
- To gain intuition and later verify deformation models based on fluid dynamics, it is often very useful to look into the time scale of the problem from a dimensional analysis point of view.

- Dimensional analysis:
$$\tau = \frac{\lambda\eta}{\gamma}$$

This reveals an interplay between viscosity (η), surface tension (γ), and feature size (λ).

- The treatment of dewetting will reveal another parameter that integrate disjoining pressure

$$\tau(k_m) = \frac{3\eta}{\gamma h_0^3 k_m^4}$$



- Viscous flow are governed by Fluid mechanics and Navier-Stokes formalism



- Let's remind the basic principles of fluids mechanics: a fluid is a substance that cannot remain resting, i.e. that flows, under a non-zero shear stress.
- Forces that act on a fluid can be seen of two nature:
 - Volume forces such as Gravity or Coriolis;
 - Surface forces at the border with a fluid (we will see some example) also act on the fluid and must be considered, sometimes as surface boundary conditions in the treatment of a fluid dynamic problem.

- The conservation of momentum can then be expressed as: $\frac{d}{dt} \int_{\Omega(t)} \rho \underline{U} d\Omega(t) = \underline{F}_e$

Where ρ is the density, \underline{U} is the velocity field, $\Omega(t)$ is the volume of fluid considered, and \underline{F}_e represent the forces acting on a fluid: $\underline{F}_e = -g \underline{e}_z - \underline{p}(x, t) \underline{n}(x, t) da + \underline{\tau}(x, t) \underline{n}(x, t) da$

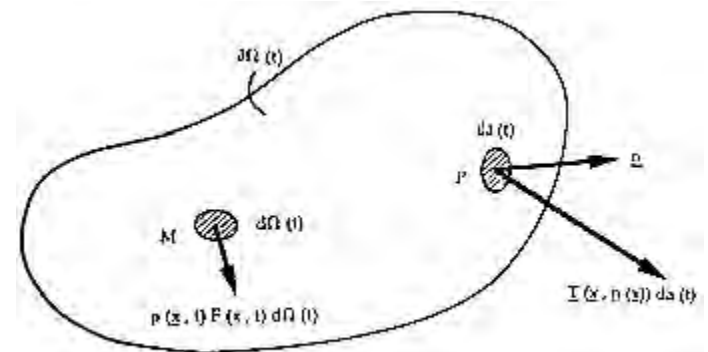
- Relation between the applied stress, the velocity field $U(x,y,z,t)$ and its derivatives via gradient and divergence, temperature, and the stress distribution inside the fluid is then;

$$\underline{\underline{\sigma}}(\underline{x}) = f(\underline{\underline{\text{grad}U}}, \rho, T)$$

$$\underline{\underline{\sigma}}(\underline{x}) = -p(\underline{x}) \underline{\underline{I}} + \underline{\underline{\tau}}(\underline{x})$$

Hydrostatic stress

Viscous stress tensor



- The local form of the conserved momentum equation is hence:

$$\rho \frac{d\underline{U}}{dt} = \rho \underline{F} - \underline{\text{grad}} p + \text{div}(\underline{\underline{\tau}})$$

- Mass conservation also imposes:

$$\frac{d\rho}{dt} + \rho \text{div} \underline{U} = 0$$

- Depending on the nature of the fluid and the flow conditions, many approximation and relations can be used.
- For example, a perfect fluid is one for which no viscous stress exist: $\underline{\underline{\tau}}(\underline{x}) = 0$
- A Newtonian fluid is an isotrope fluid for which the stress field $\underline{\underline{\sigma}}$ depends linearly on $\underline{\underline{\text{grad}}} U$

One can show that under these conditions:

$$\underline{\underline{\tau}}(\underline{x}) = \lambda (\text{div} \underline{U}) \underline{\underline{I}} + 2\mu \underline{\underline{d}} \quad \text{Dynamic viscosity}$$

Where λ and μ are called the Lamé coefficients, and we have:

Tenseur taux de déformtion:
$$\underline{\underline{d}} = \frac{1}{2} \left(\underline{\underline{\text{grad}}} U + {}^t \underline{\underline{\text{grad}}} U \right)$$

- Navier Stokes equations

Mass
conservation

$$\frac{d\rho}{dt} + \rho \operatorname{div} \underline{U} = 0$$

Cauchy
Momentum
equation

$$\rho \frac{d\underline{U}}{dt} = \rho \underline{F} - \underline{\operatorname{grad}} p + \underline{\operatorname{grad}} (\lambda \operatorname{div} \underline{U}) + 2 \operatorname{div} (\mu \underline{\underline{d}})$$

↑
Second viscosity

- Incompressible fluid

$$\operatorname{div} \underline{U} = 0$$

- Finding the right flow conditions:

- Reynolds:

$$R_e = \frac{\rho U \lambda}{\eta} \ll 1$$

Viscous forces dominate over inertia – Laminar flow

- Capillary :

$$C_a = \frac{U \eta}{\gamma} \gg 1$$

Viscous forces dominate over surface tension – slow motion and surface effect.

- Irrotational fluid: for a fluid starting static, small F and for flow in thinner confined spaces:

$$\operatorname{rot} \underline{U} = 0$$

- For a highly viscous fluid, the time derivative of the velocity is small. We can hence solve the case for which the partial derivative with time is zero.
- We suppose also the pressure to be negligible inside the film, but acting only at the surface.
- We get coupled differential equations for $\mathbf{U} = u_x \mathbf{e}_x + u_y \mathbf{e}_y$

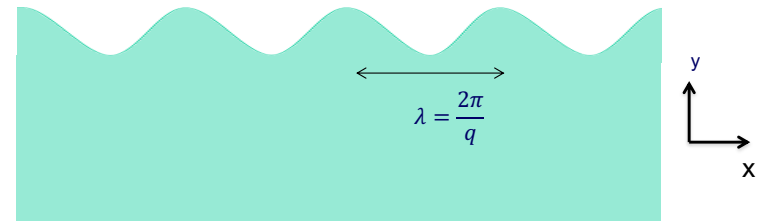
$$\frac{\partial u_x}{\partial x} + \frac{\partial u_y}{\partial y} = 0$$

$$\frac{\partial u_x}{\partial y} - \frac{\partial u_y}{\partial x} = 0$$

- By initial conditions and symmetry of the system, we can assume that the solution is periodic in x , and the velocity field exponentially decays in y .
- We can then write

$$u_x(x, y) = e^{-\alpha(d-y)} \sum_n a_n e^{inqx}$$

$$u_y(x, y) = e^{-\alpha(d-y)} \sum_n b_n e^{inqx}$$



With $y^s(x) = d + h \sin(\frac{2\pi}{\lambda} x)$ and assuming $y^s(x) - y \approx d - y$

- Plugging in the equation, we obtain that one harmonic is possible with the conditions:

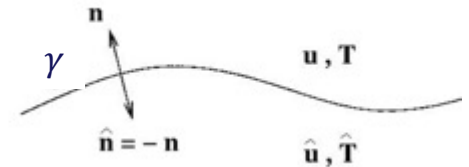
$$\alpha = q \text{ and } a_1 = i b_1$$

Without loss of generality we have:

$$u_x(x, y) = A e^{-q(d-y)} \cos(qx) \text{ and } u_y(x, y) = A e^{-q(d-y)} \sin(qx)$$

- To evaluate A , we can apply the normal-stress balance condition at the surface of the textured glass :

$$\bar{n} \cdot (\bar{\tau} \cdot \bar{n}) = \gamma \nabla \cdot \bar{n}$$



γ is the surface tension, $\bar{\tau}$ is the stress tensor and \bar{n} is the unit vector normal to the surface.

The jump in normal stress across the interface must balance the curvature force per unit area.

- From $\tau_{ij} = -p\delta_{ij} + \eta(\partial_i u_j + \partial_j u_i)$, where p is the internal pressure considered to be null, it

$$\text{comes immediately that: } \tau_{yy} = -\tau_{xx} = \frac{4\eta\pi}{\lambda} A \sin\left(\frac{2\pi}{\lambda} x\right) \exp\left(\frac{2\pi}{\lambda} y\right)$$

The normal vector to the $y^S(x)$ curve is given by : $\bar{n} = \frac{1}{\sqrt{1+(y_S'(x))^2}} (1, -y_S'(x))$. We get:

$$\bar{n} \cdot (\bar{\tau} \cdot \bar{n}) = \frac{4\eta\pi}{\lambda} A \sin\left(\frac{2\pi}{\lambda} x\right) e^{-q(y^S(x)-y)} \approx \frac{4\eta\pi}{\lambda} A \sin\left(\frac{2\pi}{\lambda} x\right)$$

- The expression $\gamma \nabla \cdot \bar{n}$ corresponds to the well-known Laplace pressure relation and linearizing using again the fact that $h \ll \lambda$, we have $\nabla \cdot \bar{n} = \partial^2 y^s(x) / \partial x^2$, which we can write

$$\gamma \nabla \cdot \bar{n} = -\gamma h \left(\frac{2\pi}{\lambda} \right)^2 \sin \left(\frac{2\pi}{\lambda} x \right)$$

Combining these two expressions in the boundary condition, one obtains:

$$\frac{4\eta\pi}{\lambda} \mathbf{A} = -\gamma h \left(\frac{2\pi}{\lambda} \right)^2 \Leftrightarrow \mathbf{A} = -\frac{\pi\gamma h}{\eta\lambda}$$

- We need now to go from a solution that considers time derivatives to be negligible, to a solution that looks into the time evolution of the roughness, in particular considering that h is a function of time;
- The surface evolution due to this velocity field can now be evaluated from a kinematic boundary condition for which the flux of volume of material across two perpendicular surfaces at positions x and $x+dx$ during a time dt equates the volume change $\Delta y^s(x) dx$ (it is understood that the third dimensions along the z direction is not shown in the derivation), which can be written as:

$$\frac{\partial y^s(x)}{\partial t} = -\frac{\partial}{\partial x} \left(\int_0^{y^s(x)} u_x dy \right)$$

which leads to:

$$\frac{\partial h}{\partial t} \sin\left(\frac{2\pi}{\lambda}x\right) = -\frac{\pi\gamma h}{\eta\lambda} \sin\left(\frac{2\pi}{\lambda}x\right) \left[\exp\left(\frac{2\pi}{\lambda}y\right) \right]_0^{y^s(x)} \approx -\frac{\pi\gamma h}{\eta\lambda} \sin\left(\frac{2\pi}{\lambda}x\right)$$

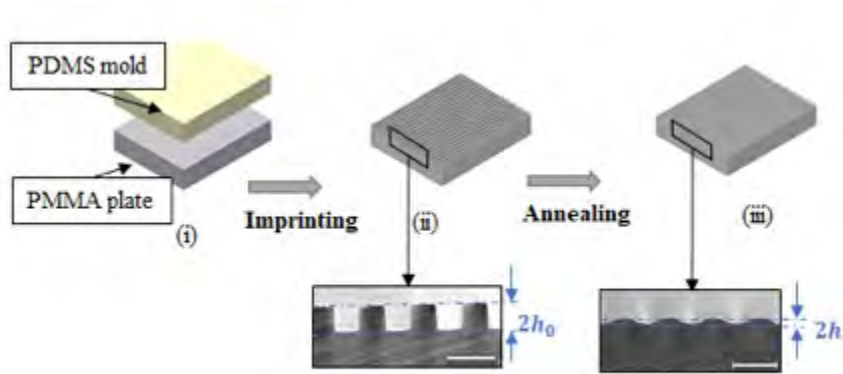
$$\frac{\partial h}{\partial t} \approx -\frac{\pi\gamma h}{\eta\lambda} \text{ or } h(t) = h_0 e^{-t/\tau} \quad \text{with} \quad \tau = \frac{\eta\lambda}{\pi\gamma}$$

- To treat the general case of any texture, we can use Fourier transform formalism in a straightforward way:

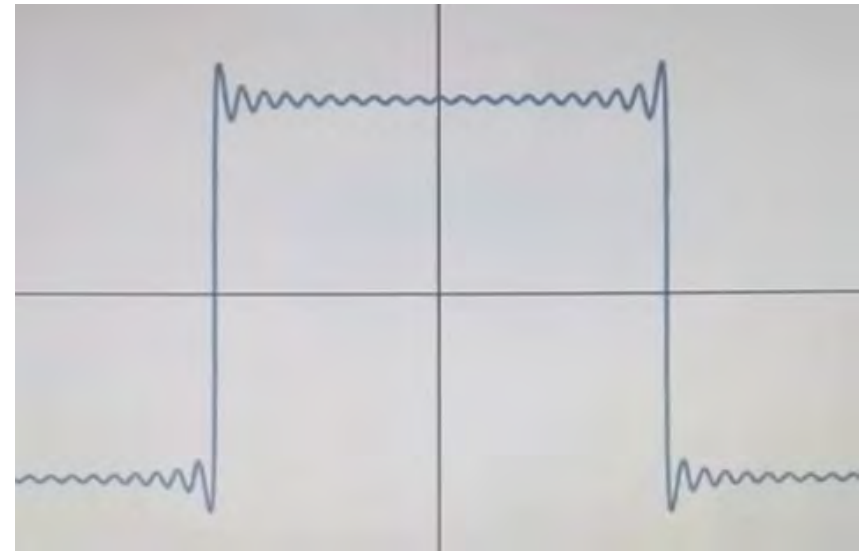
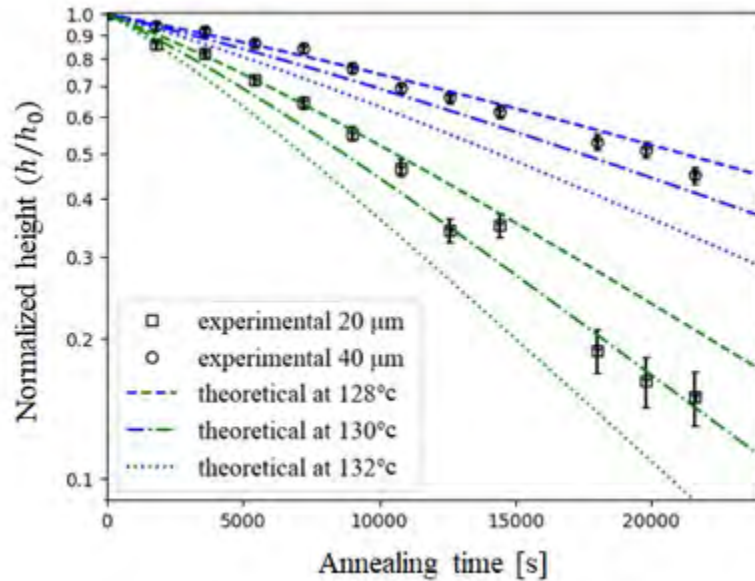
$$y(x) = \frac{4h_0}{\pi} \sum_n \frac{(-1)^n}{(2n+1)} \cos\left(\frac{2\pi(2n+1)}{\lambda}x\right)$$

$$\frac{h(t)}{h_0} = \frac{4h_0}{\pi} \sum_n \left(\frac{(-1)^n}{(2n+1)} e^{-(2n+1)\frac{t}{\tau}} \right)$$



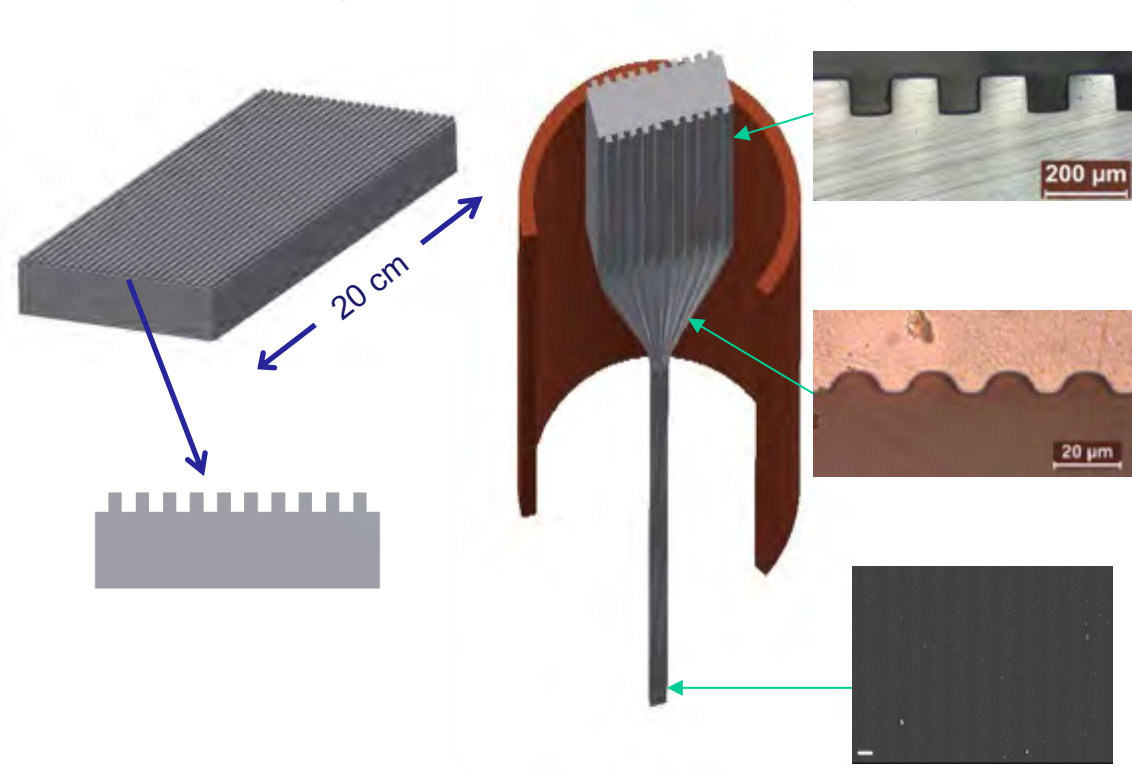


$$\tau_n = \tau/n$$



- The interplay between viscosity and surface tension can be exploited to maintain an initial texture on a polymer fiber and make textured fibers and surfaces.
- The Laplace pressure drives a reflow that collapses small textures.

Imprinting + Thermal drawing



Navier Stokes formalism:

- Incompressible Newtonian fluid
- Low Reynolds Number

$$\nabla \cdot v = 0$$

$$-\nabla \cdot p + \eta \nabla^2 v = 0$$

↖ Viscosity

Laplace Pressure: $p = \gamma \kappa$

↖ Surface tension

- Characteristic time:

$$\tau = \frac{\eta \lambda}{\pi \gamma}$$

- The model can be adapted to the thermal drawing process that is not isothermal:

- Total deformation between z and $z + dz$:

$$dh = dh_{sc} + dh_{re}$$

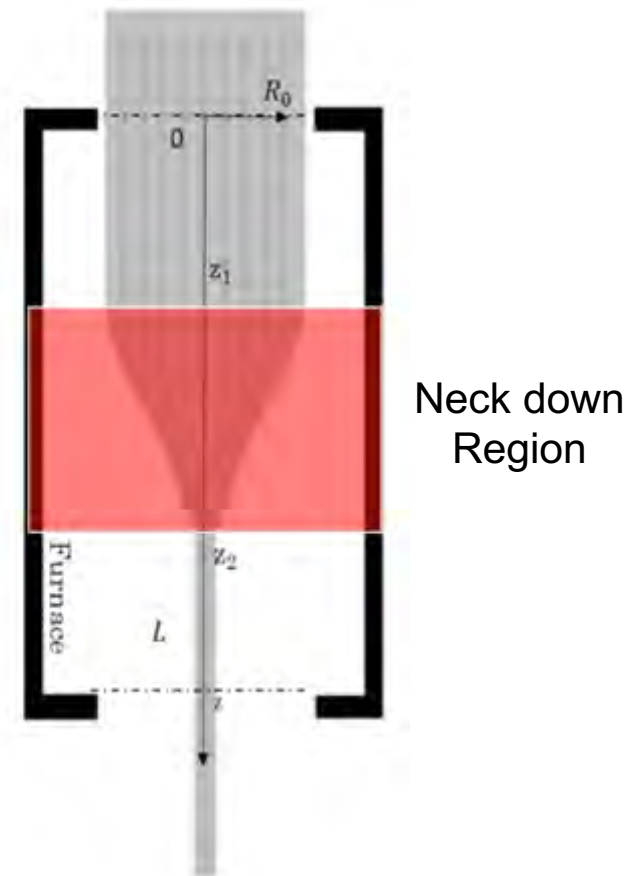
$$= -\frac{1}{2} \frac{h}{v} dv - \frac{\pi \gamma h}{\eta \lambda v} dz$$

Or

$$\frac{dh}{h} = -\frac{1}{2} \frac{dv}{v} - \frac{\pi \gamma}{\eta \lambda v} dz$$

- Final feature size of the structure on fibers:

$$h(L) = h_0 \left(\frac{v_f}{V_0} \right)^{-\frac{1}{2}} \exp \left(\int_0^L -\pi \frac{\gamma}{\eta \lambda v} dz \right)$$

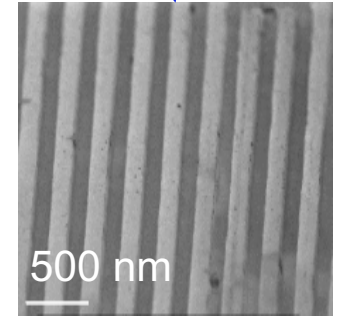
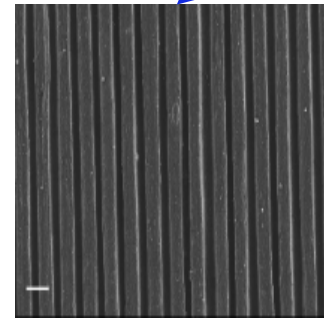
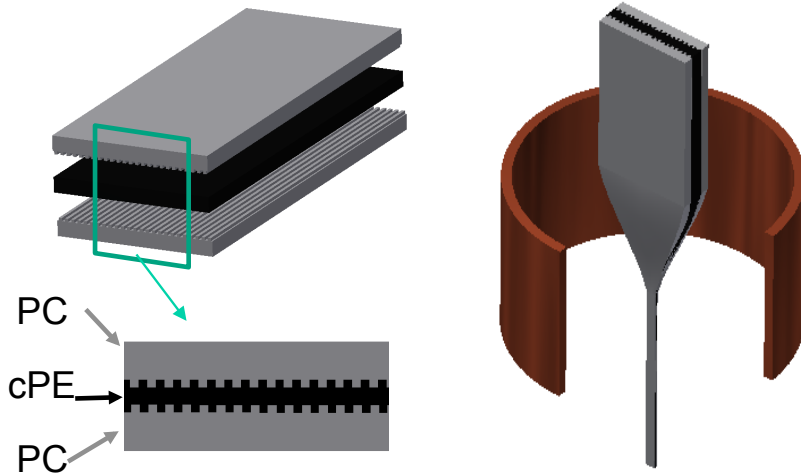


- We can also adapt it to arbitrary shapes and verify it experimentally rigorously

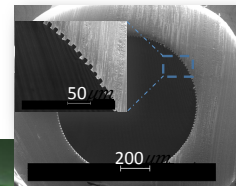
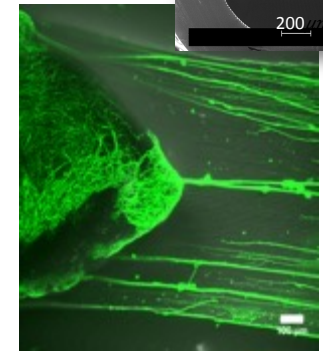
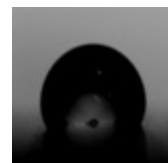
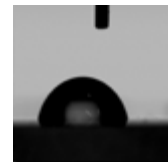
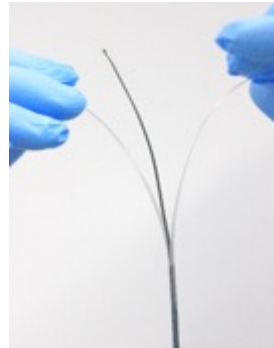
- How would you go about to prevent reflow ?
- Reduction of the interfacial energy at the texture location by adding a sacrificial polymer layer.

Characteristic time:

$$\tau = \frac{\eta \lambda}{\pi \gamma}$$



Dorsal Root Ganglia (DRG) growth within a textured hollow fiber (Prof. S. Lacour)



- What happens when we switch to a thin film configuration ?



$$P = p_L + \phi(z) - \phi(h(x))$$

- The pressure is non zero in the film, independent of y , and combines Laplace and disjoining pressure
- Let us for now consider only reflow and look into the effect of different geometry and boundary conditions on similar differential equations.

Navier Stokes formalism:

- Incompressible Newtonian fluid:

$$\nabla \cdot v = 0$$

- Low Reynolds Number:

$$-\nabla \cdot p + \eta \nabla^2 v = 0$$

↙ Viscosity

$$p = \gamma \kappa$$

- Lubrication approximation:

$$\eta \frac{\partial^2 v_x}{\partial y^2} = \frac{\partial p}{\partial x}$$

- Further hypothesis:
 - P is independent of y;
 - no slip at the substrate-film interface
 - no shear at the film-air interface

$$v_x(y) = \frac{1}{\eta} \frac{\partial p}{\partial x} \left(\frac{y^2}{2} - hy \right)$$

- The surface evolution due to this velocity field can now be evaluated from a kinematic boundary condition Mass conservation:

$$\frac{\partial h}{\partial t} = - \frac{\partial}{\partial x} \left(\int_0^h v_x dy \right) \quad \frac{\partial h}{\partial t} = \frac{1}{3\eta} \frac{\partial}{\partial x} \left(h^3 \frac{\partial p}{\partial x} \right) \quad \text{and} \quad p \approx \gamma \frac{\partial^2 h}{\partial x^2}$$

$$\frac{\partial h}{\partial t} = \frac{\gamma}{3\eta} \frac{\partial}{\partial x} \left(h^3 \frac{\partial^3 h}{\partial x^3} \right)$$

- Let us now study the evolution of a small perturbation ($\varepsilon \ll h_0$) evolving at the fluid surface with a wavenumber k and amplitude $\varepsilon(t)$:

$$h(t) = h_0 + \varepsilon(t) \cdot \sin(qx)$$

- At the initial stage of the flow, when $h(x)$ is still comparable with h_0 , we can linearize

$$\frac{\partial \varepsilon}{\partial t} \propto -\frac{\gamma h_0^3}{\eta \lambda^4} \varepsilon(t)$$

- We can identify the time scale associated with the initial stage of reflow:

$$\tau \sim \frac{\lambda^4}{\gamma h_0^3} \eta$$

- Here again, a very similar form of the interplay between viscosity and surface tension !
- If we had no other forces acting upon the film, the roughness / texture on the film would also disappear.
- The case we consider however has very thin layers where Van der Waals forces acting at the film interfaces, with the substrate and with air, are no longer negligible.

- What happens when we switch to a thin film configuration ?



$$P = p_L + \phi(z) - \phi(h(x))$$

- The pressure is non zero in the film, independent of y , and combines Laplace and disjoining pressure.
- One can keep the same analysis as before, but this time the pressure has an extra term:

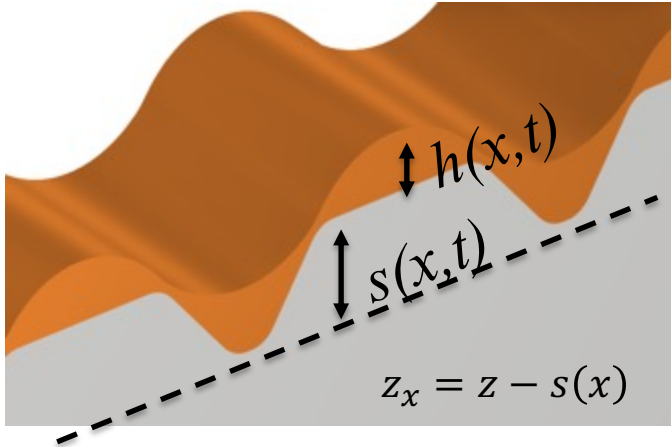
$$\frac{\partial h}{\partial t} = -\frac{1}{3\mu} \nabla \cdot (h^3 \nabla (\gamma \nabla \kappa - \Pi(h)))$$

- This extra term will be significant when the film is thin enough
- Even if the film is thick, there is a way to control where the film gets thin and can be destabilized: template dewetting.



- The film is deposited on a textured substrate and conforms initially to the substrate. Has we heat up, the film first flows under the effect of Laplace pressure. The flow of matter makes the film very thin at the top of the pyramids, where it destabilizes and can be subject to break-up.
- The film then adopts its equilibrium shape.

- The treatment of the textured substrate complicates a bit the mathematics of it.



$$h(t) = h_0 + u(t) \cdot \sin(Kx) \quad K = \frac{2\pi}{\lambda_r}$$

Effect of the substrate shape:
 $\zeta(x, t) = h_0 + (u(t) + S_0) \cdot \sin(Kx)$

$$p_L(x) = \gamma \kappa = -\gamma \partial_{z_x z_x} (h + s) \quad \text{Linearized curvature}$$

$$v_z(z_i = 0) = 0 \quad \text{No slip}$$

$$\partial_{z_x} v_x(z_x = h) = 0 \quad \text{No shear stress}$$

$$\partial_{z_x} P = 0 \quad \text{P constant in the film}$$

- The assumptions we made earlier hold:
 - Newtonian incompressible flow
 - Inertie is neglected (high viscosity)

- With these notations, we can re-write the governing flow equation:

$$\partial_t h + \partial_x \left(\frac{h^3}{3\eta} \cdot \partial_x (\gamma \cdot \partial_{xx} (h + s) + \phi(h)) \right) = 0$$

- Ignoring for now the intermolecular forces: $\partial_t u = -\frac{\gamma h_0^3}{3\eta} K^2 [(K^2)u(t) + S_0 K^2]$

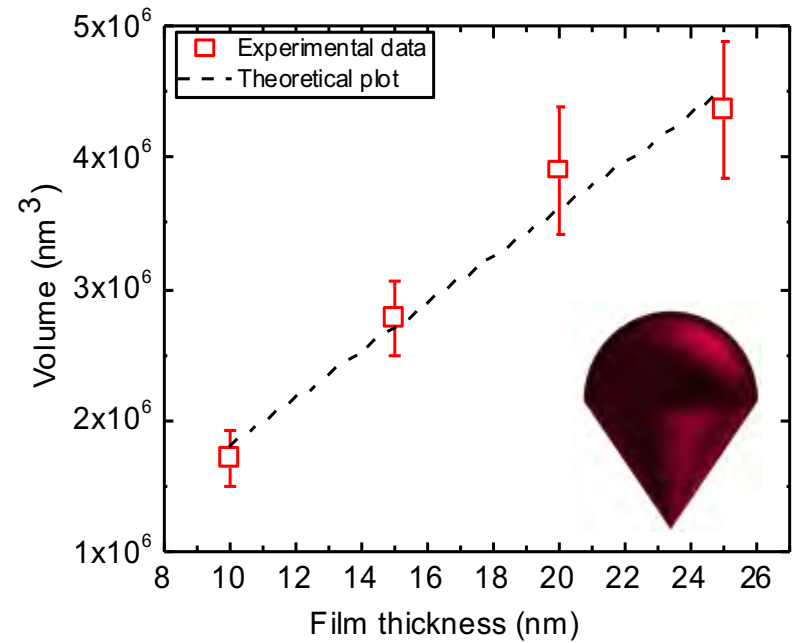
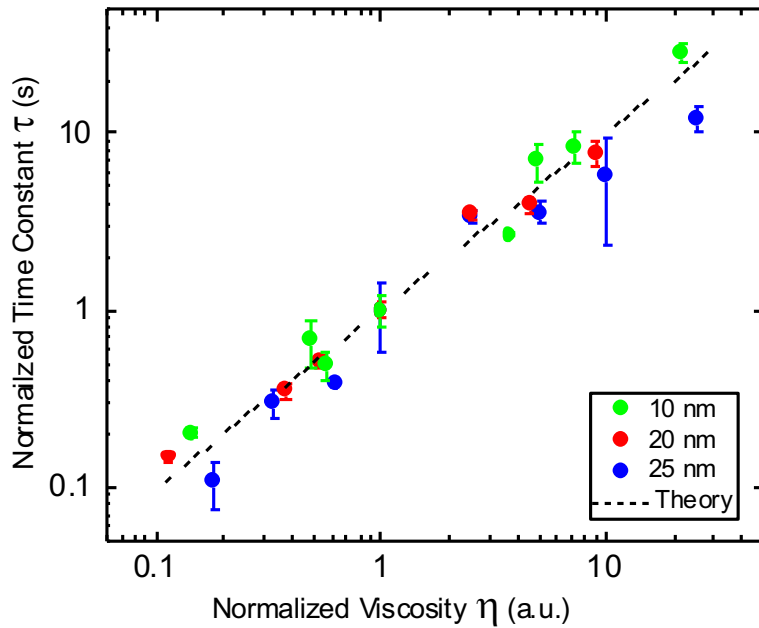
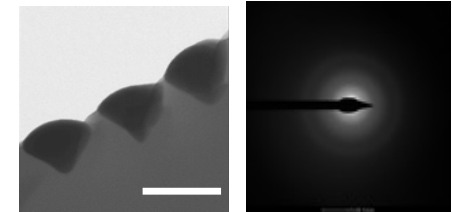
- Which leads to: $u(t) = S_0 (e^{-\frac{t}{\tau_r}} - 1)$ and $\tau_r = \frac{3\eta}{h_0^3 \gamma K^4}$

- Considering the simple case of one harmonic: $h(x, t) = h_0 + \varepsilon(t)\sin(qx)$



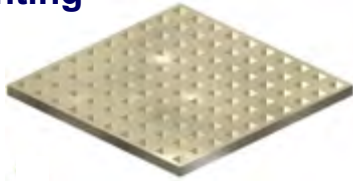
$$\frac{\partial \varepsilon}{\partial t} \propto -\frac{\gamma h_0^3}{\eta \lambda^4} \varepsilon(t)$$

$$\tau \sim \frac{\lambda^4}{\gamma h_0^3} \eta$$

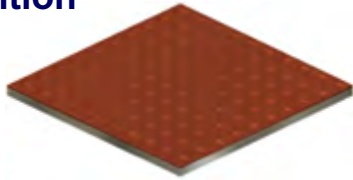


Constant volume

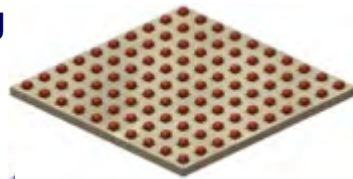
Nano-imprinting



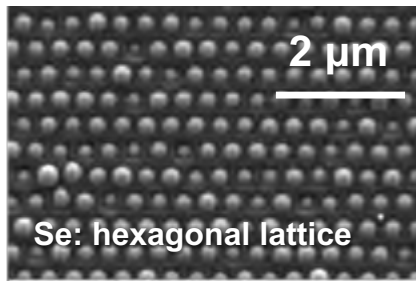
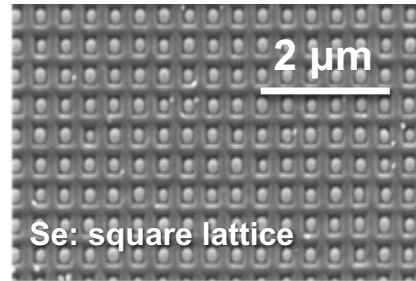
Film deposition



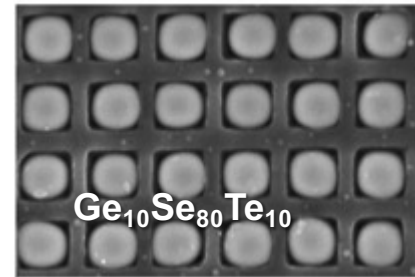
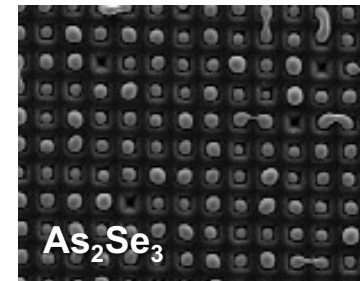
Dewetting



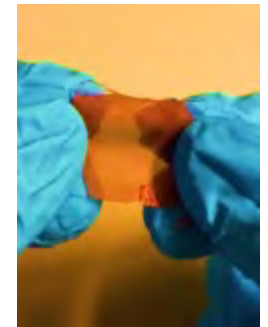
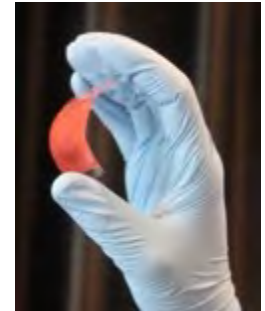
Our process enables...



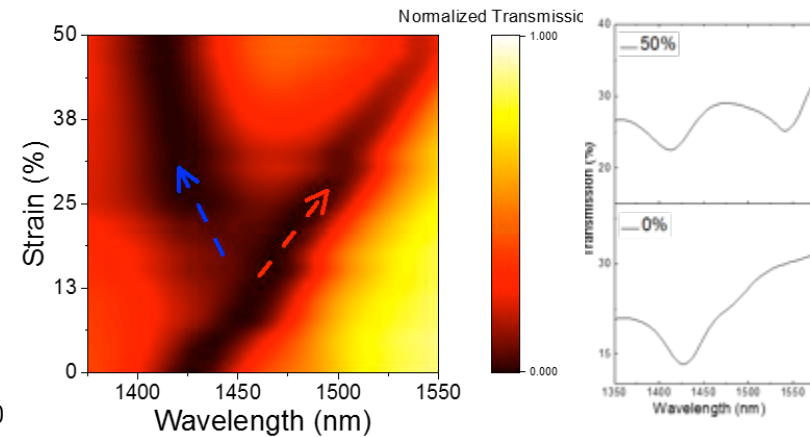
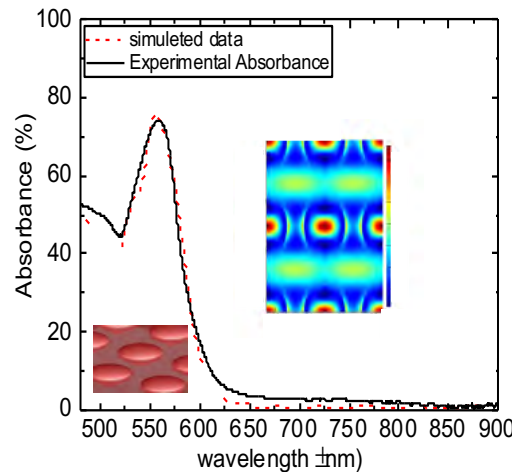
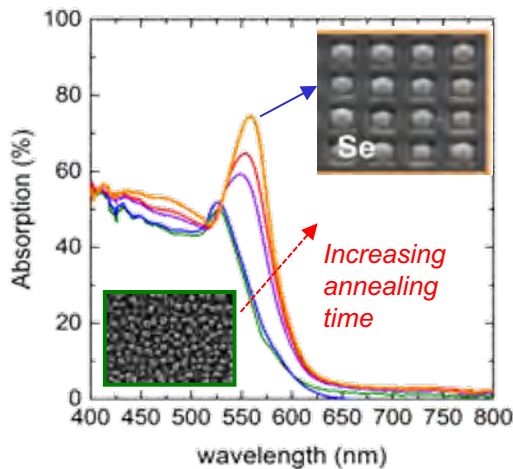
Different structures



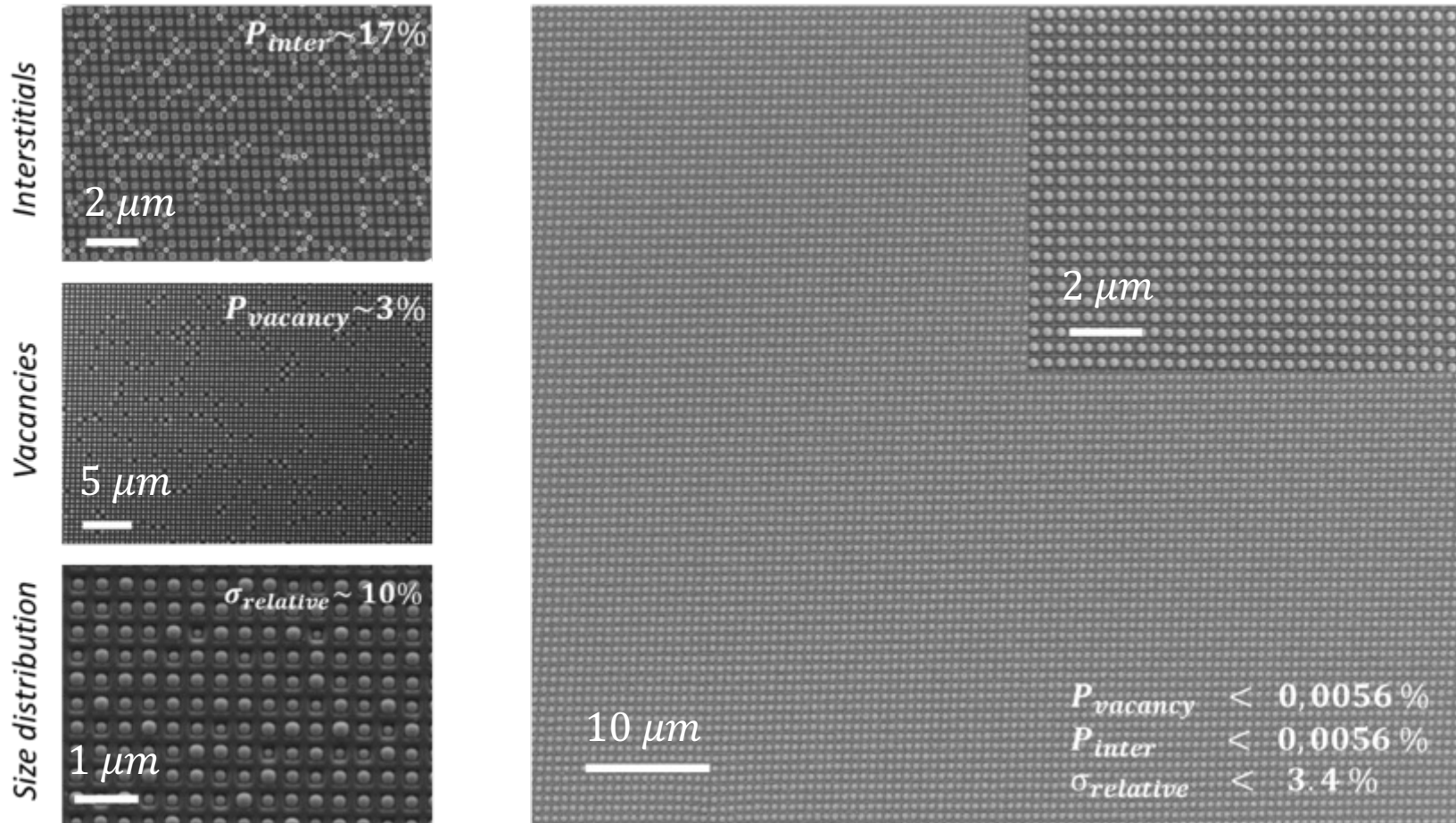
Different Materials

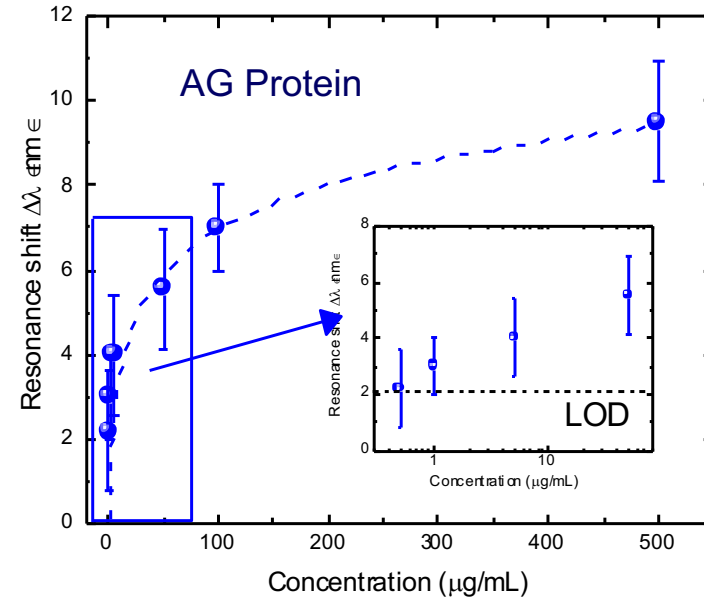
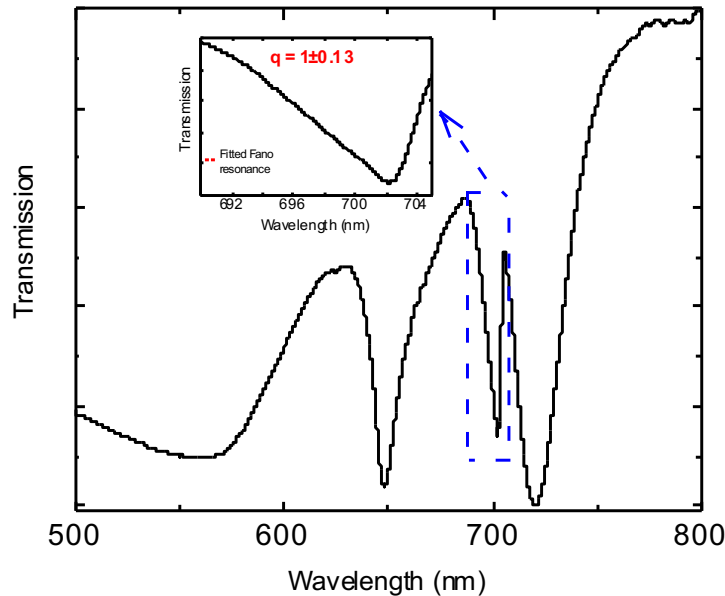
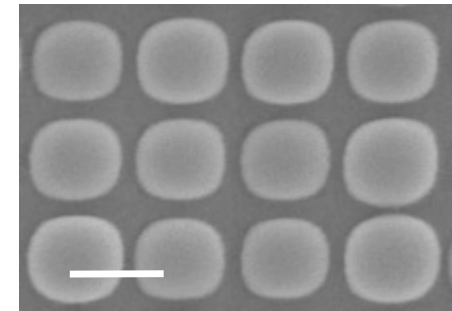
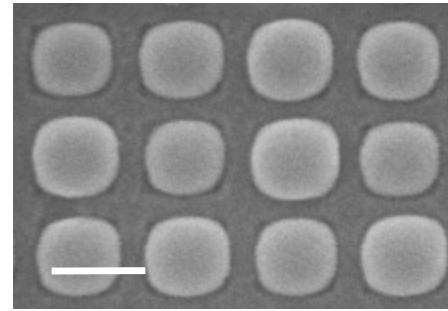
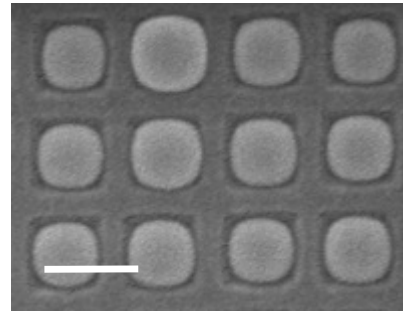
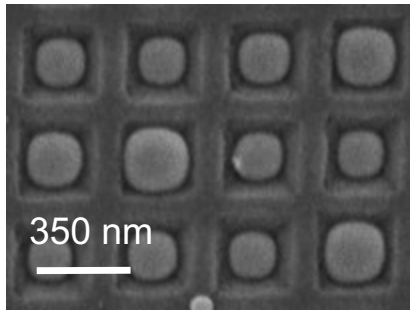
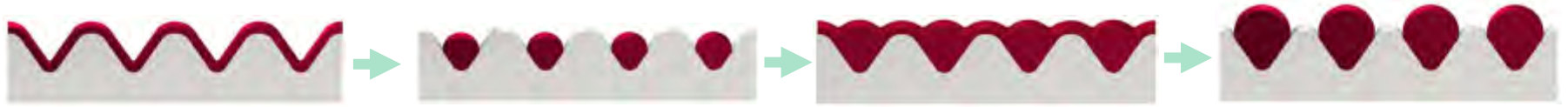


Different Substrates



- Optimizing the pattern and materials can lead to almost defect free structures over very large areas.





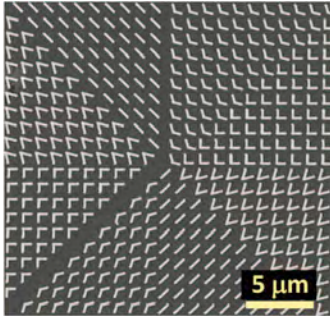
Highlighted in a "News and Views" in Nature Nanotechnology (Prof. Hu, MIT)

T. Das Gupta et. al., Nature Nanotechnology 14, 320 (2019)

Collaboration with Prof. Altug

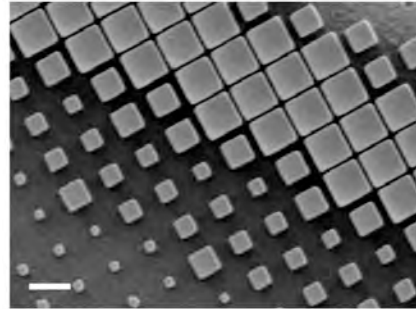
- All-dielectric metasurfaces constitute promising candidates for the next generation of photonic nanostructured devices.

- Phase discontinuity metasurface



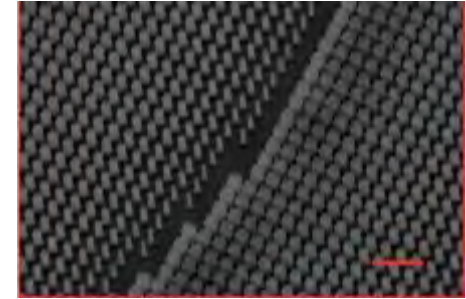
Yu et al, Science 2011

- Achromatic metalens



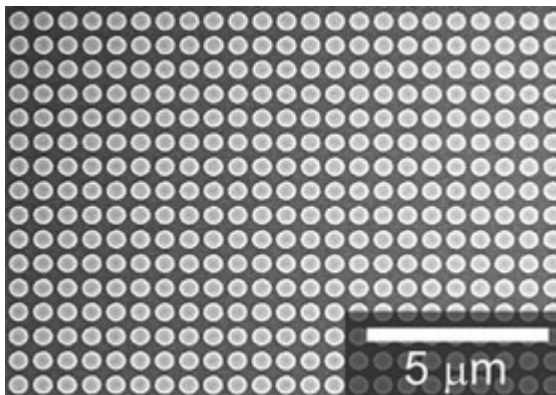
M. Khorasaninejad et al, Nanoletters, 2016

- MEMS tunable dielectric metasurface lens



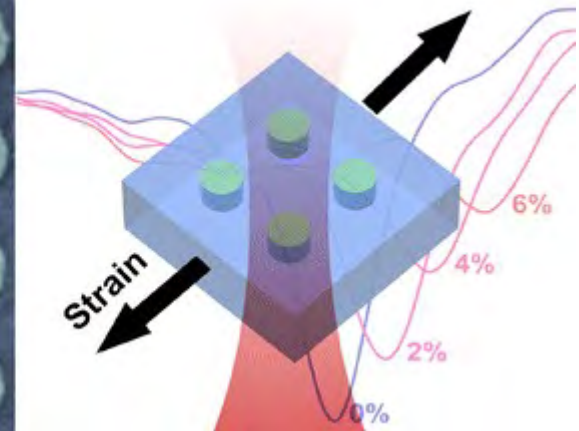
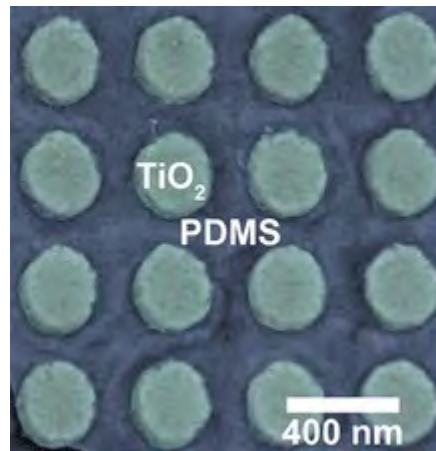
Arbabi et al, Nature Communication, 2018

- All dielectric Huygens metasurface



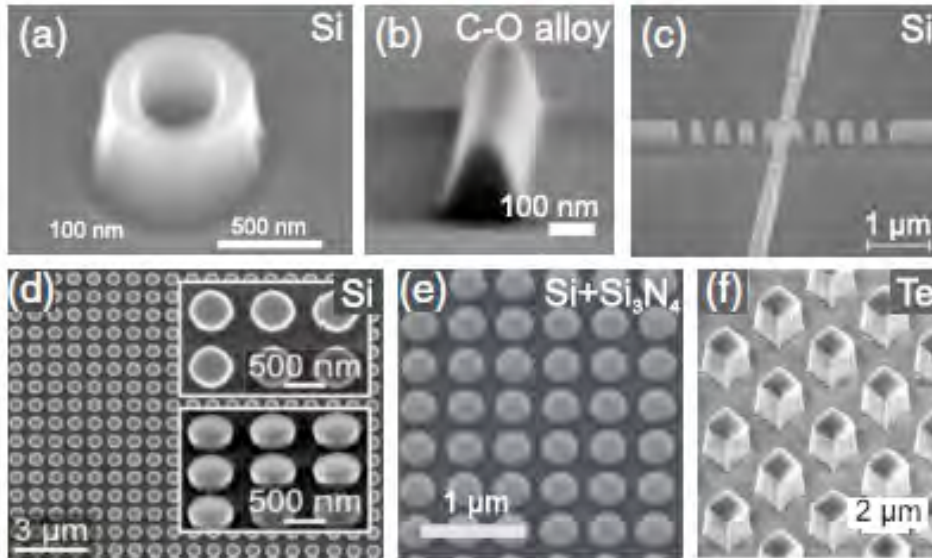
Dekker et al, Adv Opt Mat 2015

- Mechanically tunable metasurface



Gutruv et al, ACS Nano 2016

- It remains challenging to fabricate nanostructured metasurfaces using lithography approaches
- Disruptive technologies emerge thanks to the combination of the proper device concepts, materials AND processes.

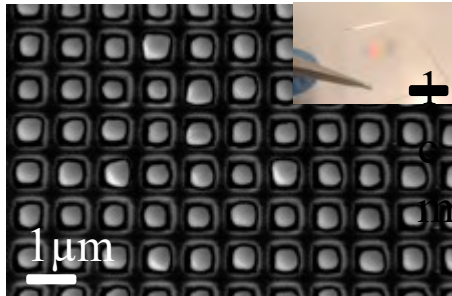


Baranov. et al., *Optica*, 2017

- Costly and complex
- Not adaptable to soft substrates
- Limited to wafer scale
- Hard to fabricate spherical particles
- Roughness

Our vision: understand and engineer fluid instabilities of nano-scale optical glass layers to self-assemble in a simple way efficient metasurfaces at large scale and over arbitrary surfaces

- Large-area meta gratings for refractive index sensing: *manuscript in preparation*
 - We reduce the index of the substrate
 - Reducing the index of the substrate increases sensitivity by pushing the resonating field away from the substrate



330nm/RIU

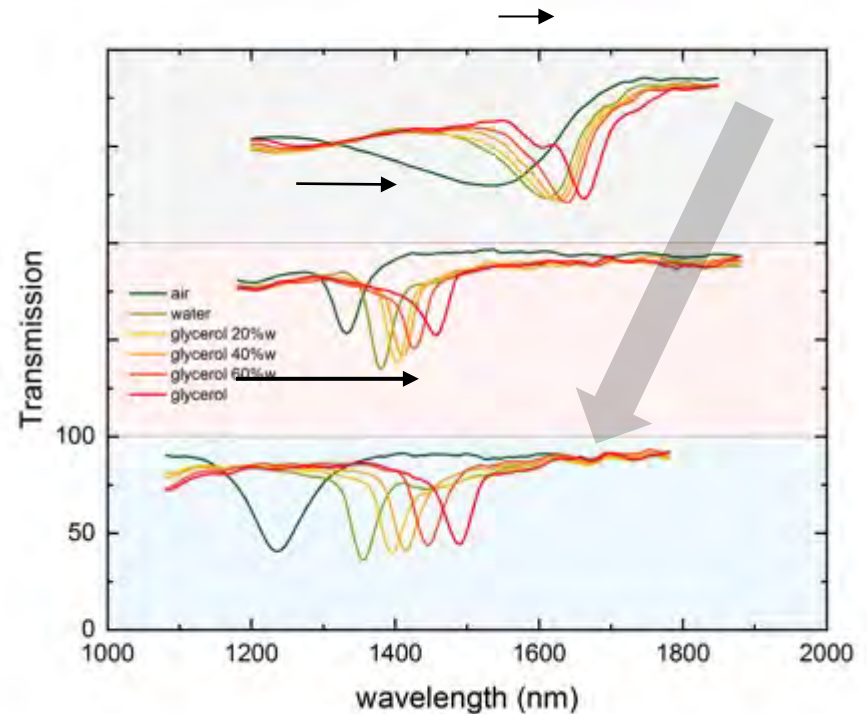
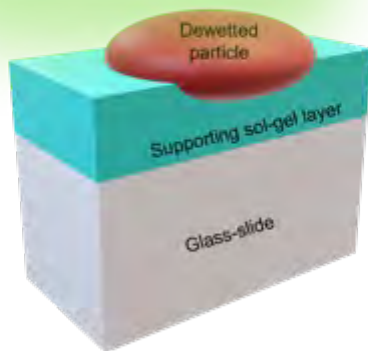


513nm/RIU

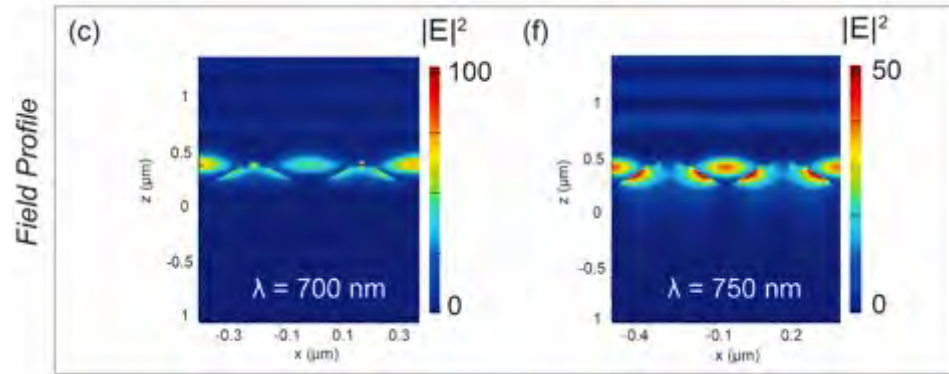
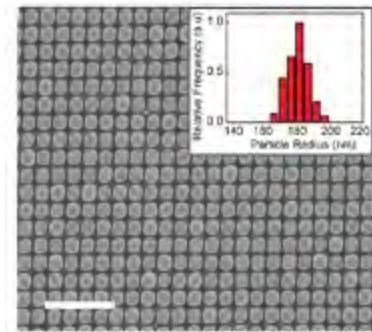


934nm/RIU

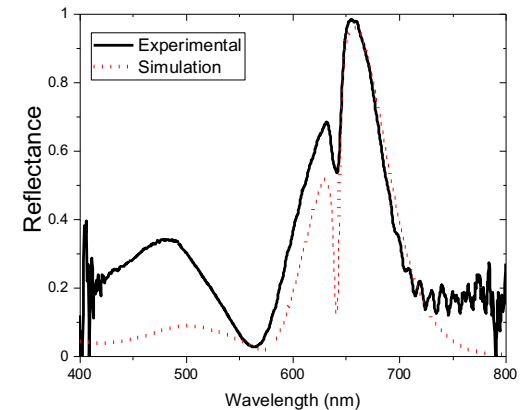
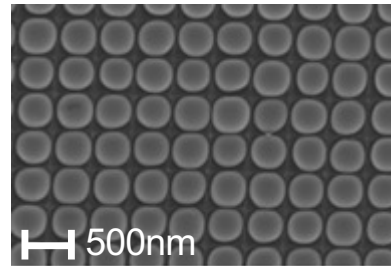
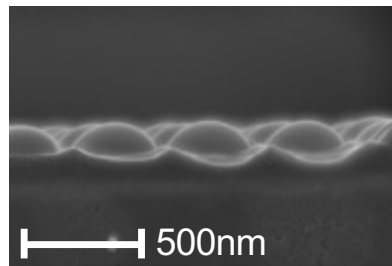
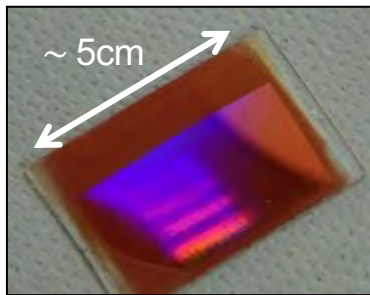
Varying bulk refractive index



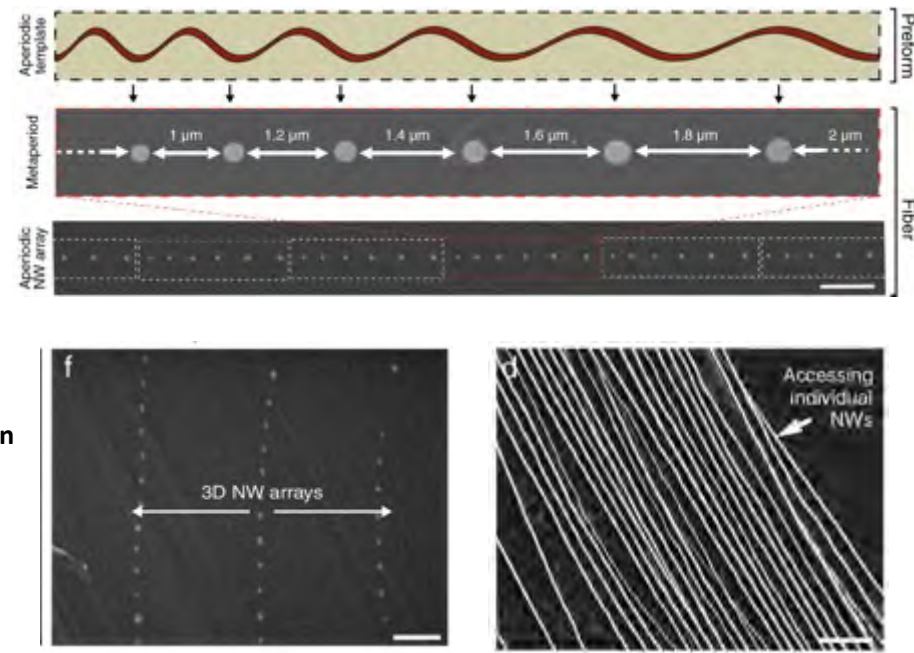
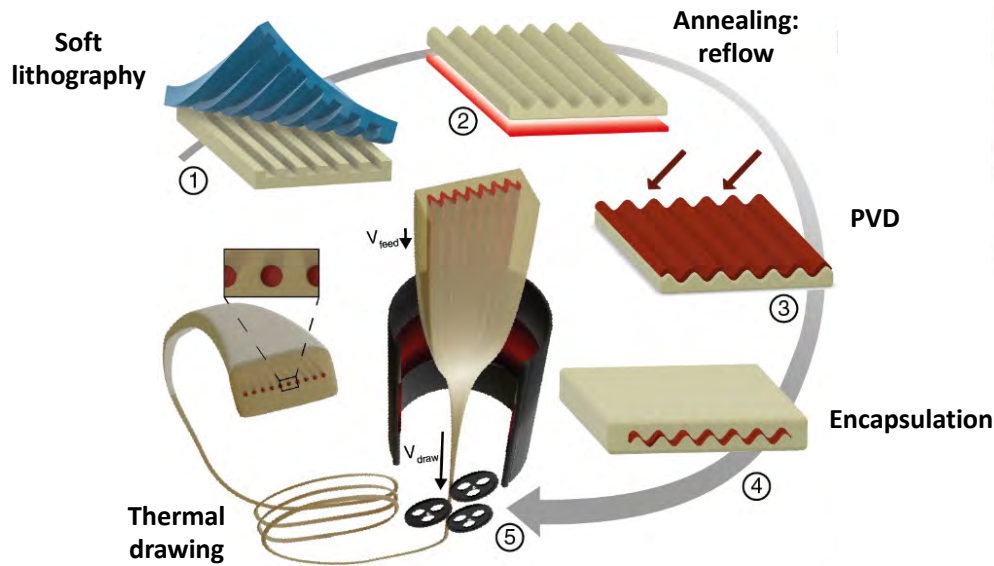
- Architectures for Non-linear optics: T. Das Gupta et. al., *Nanophotonics*, 10, 3465 (2021)

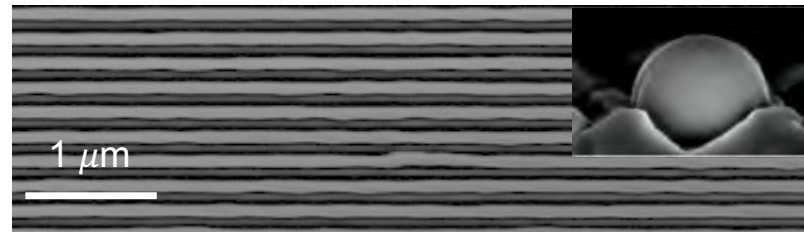
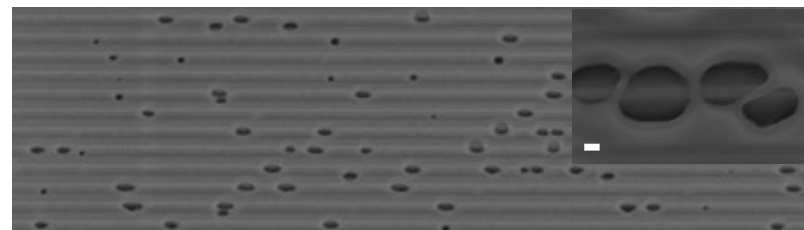
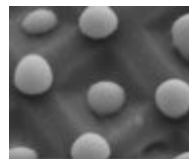
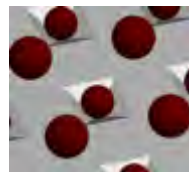
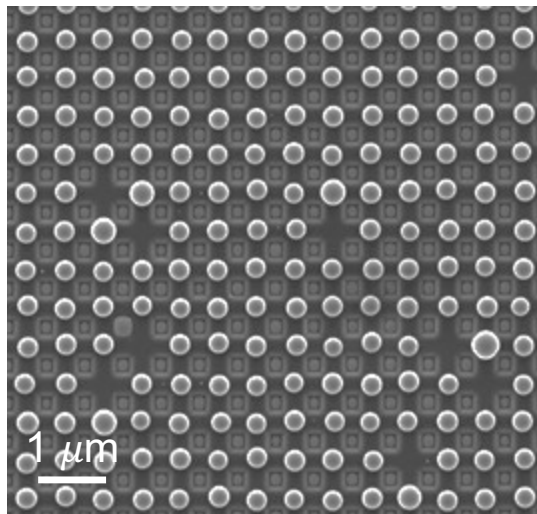
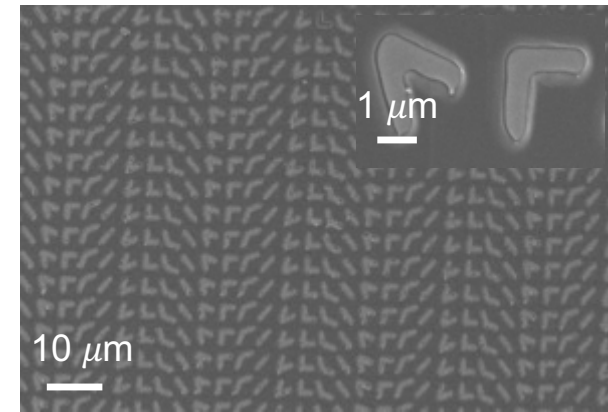
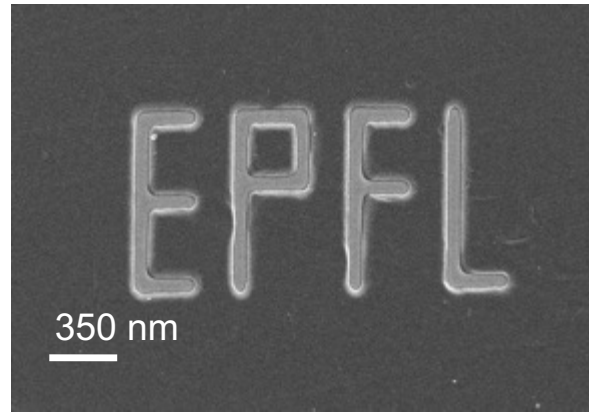
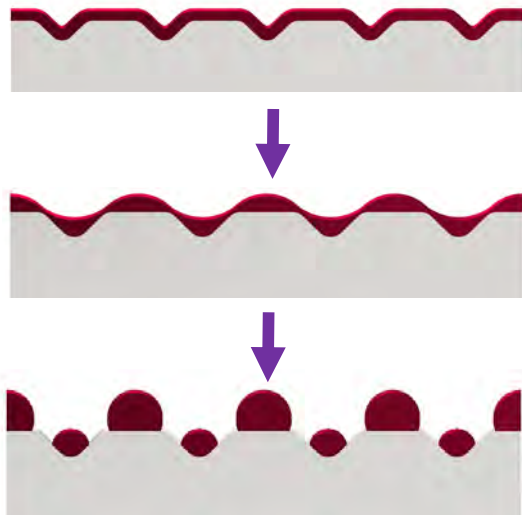


- Omnidirectional Metareflector at optical frequencies: *Manuscript in preparation*

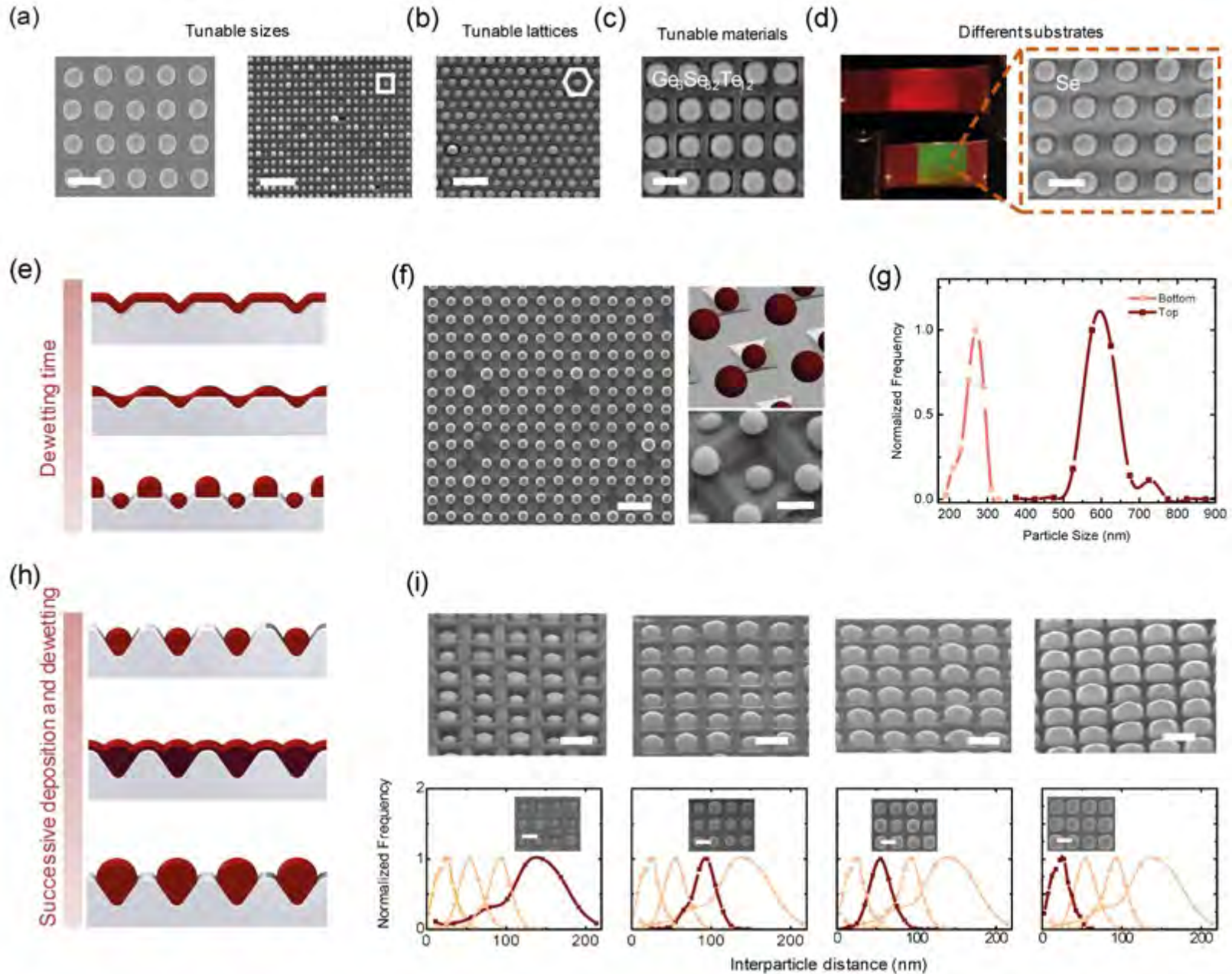


- Recently, we could combine template dewetting with thermal drawing.
- We can maintain very long nano-wires as the stretching process smoothens out the fastest growing perturbation.

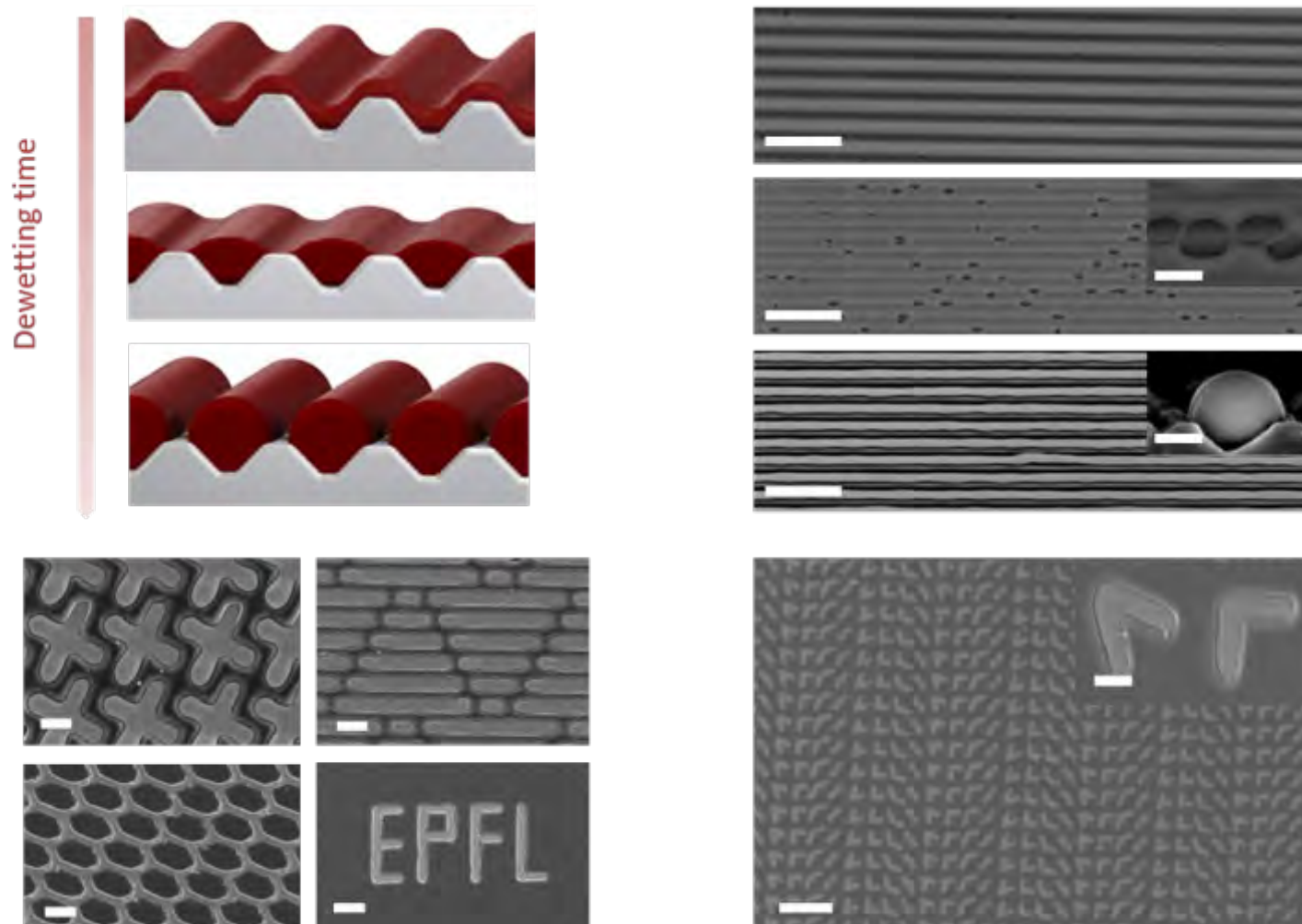




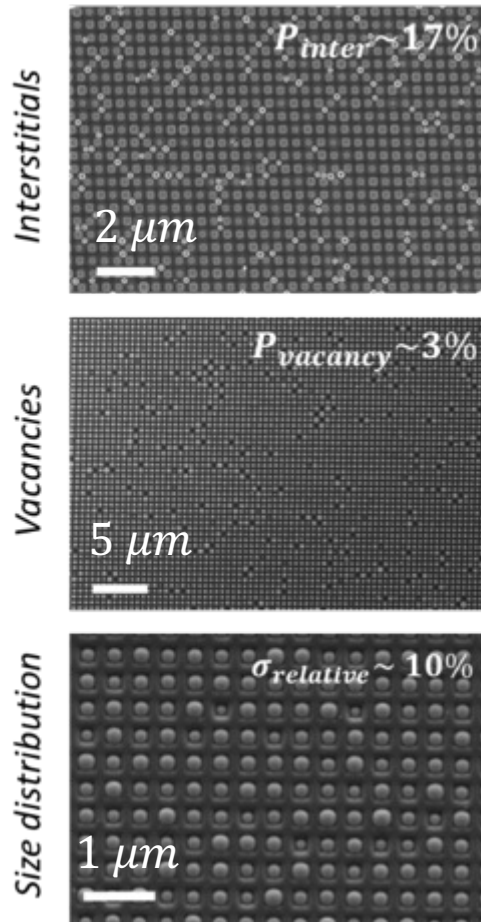
- Metasurfaces
- Photonic circuits
- Energy harvesting
- SHG
- Bio-sensing
- ...



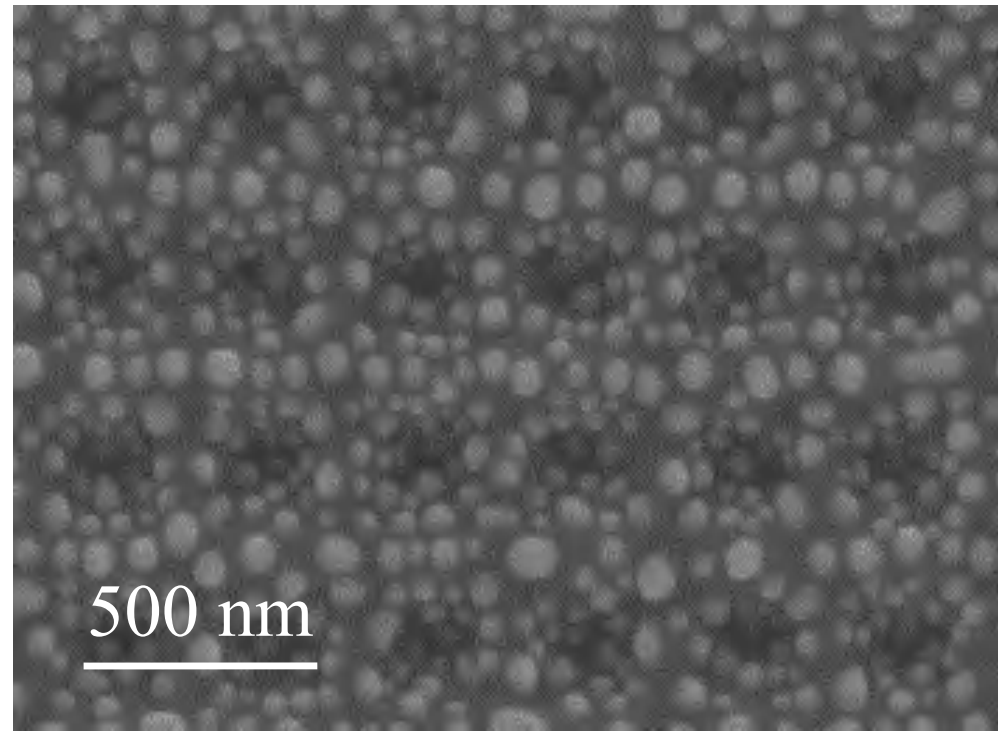
- Other shapes that can be elongated can also be generated.



- Very thin films turn out to not lead to an ordered dewetted pattern.

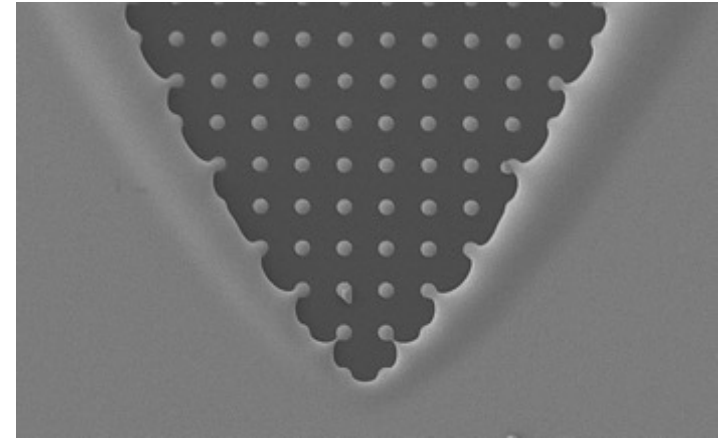
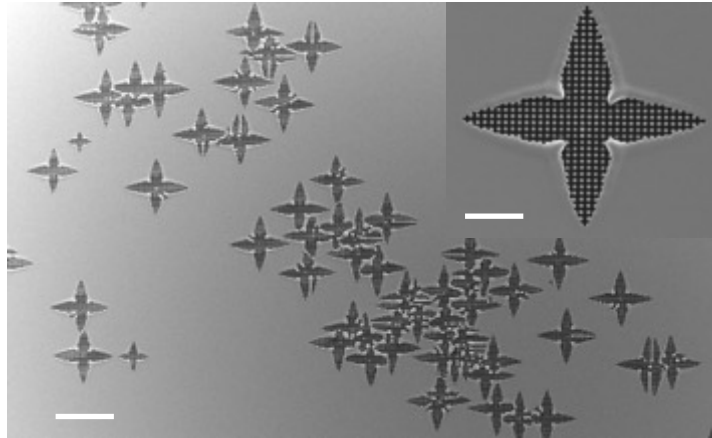


$$\tau_r \gg \tau_{sp}$$

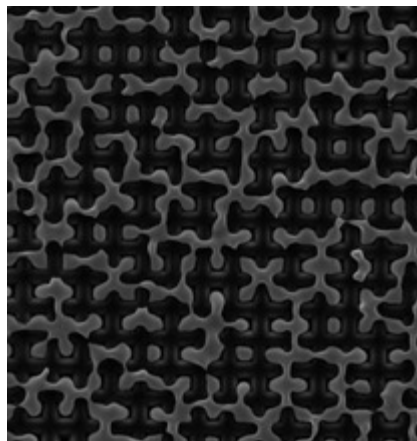


- Other patterns requires to go deeper in our understanding of not just the reflow but also the dewetting aspect.

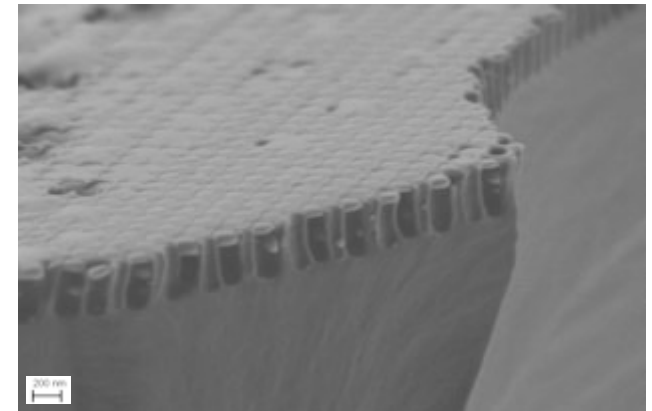
Thicker films:



Intermediate dewetting time:



High aspect ratio structures:



- We will do an analytical approach by linearizing and simplifying the problem, and considering short times
- We will then present a modeling study that treat

- Dewetting can unfold according to two main mechanisms:
 - It can nucleate at random defect points: heterogeneous nucleation
 - Capillary waves can be amplified on the film surface: spinodal dewetting

- Let us for now consider spinodal dewetting, and come back to the model above, this time not neglecting the contribution of the disjoining pressure.

$$\partial_t h + \partial_x \left(\frac{h^3}{3\eta} \cdot \partial_x (\gamma \cdot \partial_{xx} (h + s) + \phi(h)) \right) = 0$$

- A first way to get an intuition of the competition between the different mechanism that induce fluid flow, is to take a linearization approximation of the perturbation, the laplace pressure and the disjoining pressure.
 - $h(t) = h_0 + \varepsilon(t) \cdot \sin(kx)$ with $\varepsilon \ll h_0$
 - $\partial_{xx}(h + s) \sim -\gamma k^2$
 - And at the initial stage: $\partial_x \phi(h(x)) \sim \partial_x \phi(h_0)$

Which leads to:

$$\partial_t \varepsilon = \frac{h_0^3}{3\eta} k^2 (-\gamma k^2 + \partial_x \phi(h_0)) \varepsilon(t) + O(\varepsilon^2)$$

$$\frac{\partial \varepsilon(t)}{\partial t} = \frac{h_0^3}{3\eta} k^2 \left(-\gamma k^2 + \frac{\partial \phi}{\partial x}(h_0) \right) \varepsilon(t)$$

- The stability of the film essentially depends on the sign of the Van der Waals potential:
 - If, $\partial_x \phi(h_0) < 0$, then the perturbation is damped for all wavevectors k and the film is stable.
 - However, if $\partial_x \phi(h_0) > 0$, there can exist a range of wavevectors $0 < k < k_c$ for which a perturbation is amplified.

$$k_c = \sqrt{\frac{1}{\gamma} \frac{\partial \phi}{\partial x}(h_0)}$$

- We can then identify the time scale associated with the initial stage of spinodal dewetting:

$$\tau_{sp} = \frac{3\eta}{\gamma h_0^3 k^2 (k_c^2 - k^2)}$$

- In spinodal dewetting conditions ($0 < k < k_c$ and $\partial_x \phi(h_0) > 0$), pinch-off is due to the growth of a particular wavelength λ_m .
- The spinodal instability time scale associated to this characteristic wavelength λ_m may thus be rewritten :

$$\tau_{sp}(k_m) = \frac{3\eta}{\gamma h_0^3 k_m^4}$$

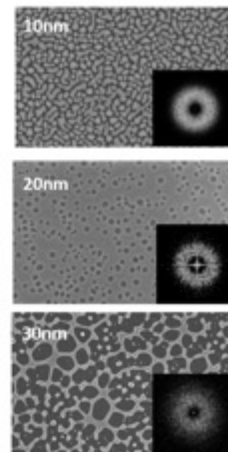
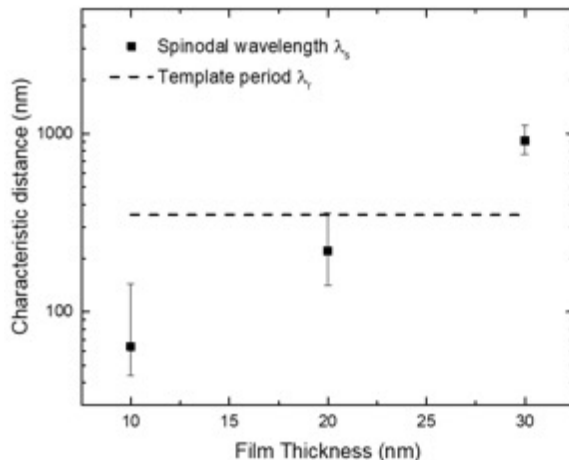
- Spinodal dewetting and thermal reflow have competing effects, which we assumed unfold independently, and one will dominate depending on its time scale

$$\tau_r = \frac{3\eta}{h_0^3 \gamma K^4} \propto \lambda^4$$

$$\tau_{sp}(k_m) = \frac{3\eta}{\gamma h_0^3 k_m^4} \propto \lambda_m^4$$



- To be able to compare these time scales, we need to be able to evaluate the characteristic spinodal dewetting wavelength (λ_m), which is very hard to model or access theoretically.
- Instead, we turn to evaluate an experimental value of λ_m that varies significantly with the initial film thickness, and compare it to λ , the wavelength of the pattern.
- We used FFT of the SEM image to extract a characteristic length of initial dewetting.



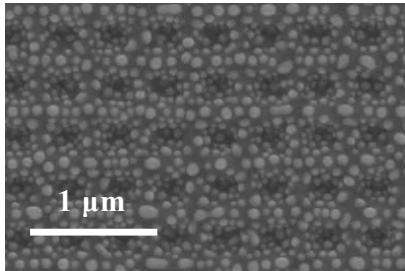
- Thin films of SeTe different thicknesses are deposited on a flat substrate.
- For $h_0 < 15$ nm no percolation !

Is continuum Mechanics appropriate ?

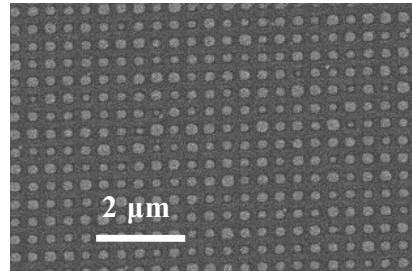
- For h_0 around 20 nm, the wavelengths are comparable but the amplitude of reflow
- For $h_0 > 30$ nm, reflow will initially dominate, leading to ordered dewetting.

- To verify this approach experimentally, we deposited films on a textured substrate with a period λ of 350 nm.

10 nm SeTe



20 nm SeTe



30 nm SeTe

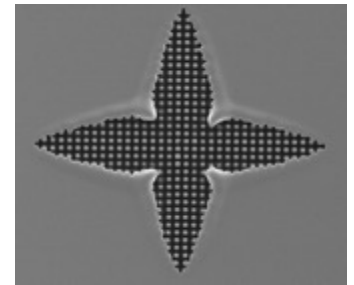
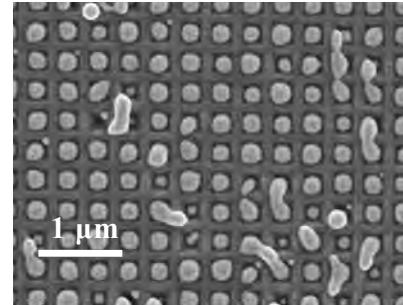
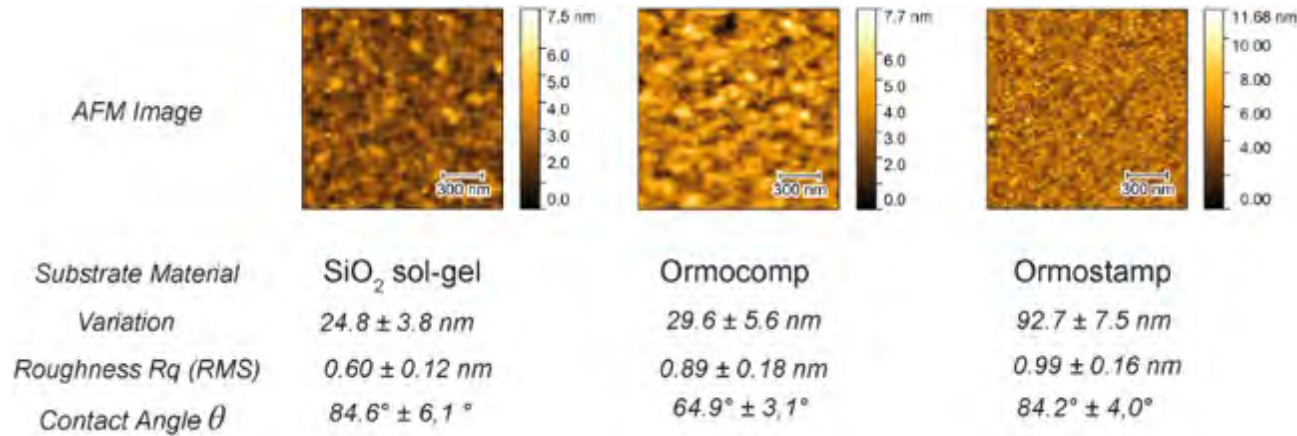


Table 1 - Time evolution of a SeTe film over a 350 nm period square inverted pyramid lattice.

- These results validate to a large extent our simplified model.
- These are representative dewetting patterns. However, this is quite dependent on the quality of the surface, its roughness and possible surface treatment.
- We consider different types of substrates:
 - Sol-gels based on acid-catalyzed Methy(triethoxysilane), followed by a pyrolysis step at 400° C,
 - Thermoplastic polymers such as polycarbonate, which exhibit ultra-low surface roughness due to reflow above their glass transition temperature,
 - UV-curable commercial resins, in particularOrmocomp and Ormostamp from Microresist, Germany.

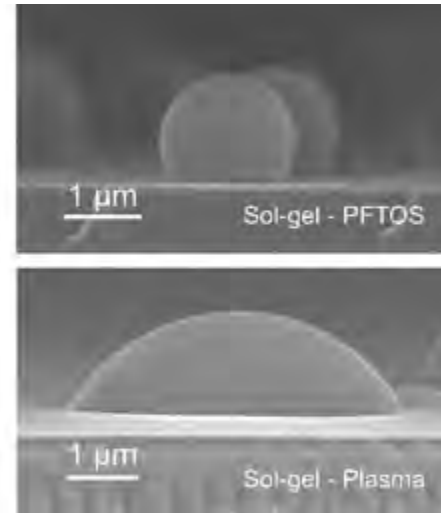
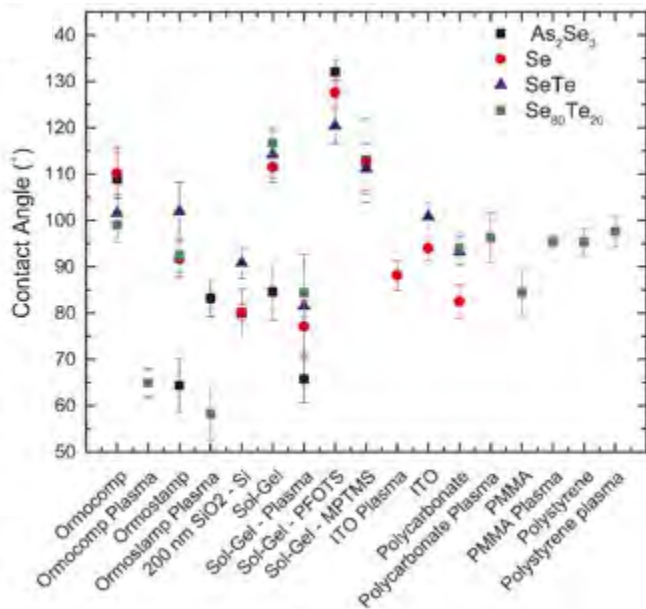
The pyrolysis step for sol-gels helps to densify the resulting silica structure, while pyrolyzing residual organic components.

- Substrate preparation is also essential:
 - Surface roughness* must be minimized: All root mean squared (RMS) roughness values are inferior to 1 nm, which, although not competitive with typical Si wafer roughness, compares favorably with most other surfaces.



- Substrate preparation is also essential:
 - Cleaning*:
 - thorough cleaning the substrates to remove any chemical inhomogeneities is a critical step to insure a homogeneous substrate surface energy, and consequently homogeneous dewetting patterns.
 - The use of polymers largely restricts the use of aggressive solvents such as H₂SO₄ or HF, commonly used to clean traditional wafers such as. It also helps to wash away nanoimprinting residues such as silicone oil traces from the PDMS or other contaminants, All substrates are subsequently washed systematically using isopropanol (degreasing agent), ethanol, and water.

- To control the protocol for preparing the substrates, we can measure the standard deviation on the contact angle obtained from SEM micrographs.
- The error bars stem from a combination of imaging analysis related uncertainties and substrate surface roughness, which induce local triple line pinning and deviation for equilibrium contact angle.



- Different treatment can also influence the interaction between the glass film and the substrate:
 - Silanes, using Trichloro(1H,1H,2H,2H-perfluorooctyl)silane (labelled PFOTS) or (3-Mercaptopropyl)trimethoxysilane (MPMTS). PFOTS is known to largely increase the hydrophobicity of silicon wafers, while MPMTS is a well-know adhesion promoter.
 - Plasma treatment: a short oxygen treatment lowers interfacial tension and the contact angle.

This is key to slow the growth of holes from defects and ensure an homogeneous dewetting.

- To better take into account the effect of the substrate and of the intermolecular forces via the disjoining pressure, we need to turn to a numerical analysis.
- The pressure is non zero in the film, independent of y , and combines Laplace and disjoining pressure.

$$P = p_L + \phi(z) - \phi(h(x))$$

- One can keep the same analysis as before, but this time the pressure has an extra term:

$$\frac{\partial h}{\partial t} = -\frac{1}{3\mu} \nabla \cdot (h^3 \nabla (\gamma \nabla \kappa - \Pi(h)))$$

μ is the dynamic viscosity, and Π the disjoining pressure.

- I will also move away from an analytical analysis that obviously has limitations, especially regarding the linearization of the curvature, and now the treatment of the disjoining pressure.
 - However, I always encourage to confront experiments, models and systems first with an analytical approach even simplified, to develop an intuition on a systems and reveal influential parameters that cannot be neglected.
- The disjoining pressure gathers the influence of intermolecular forces and derives from from a potential.

- The disjoining pressure term is assumed to stem from a classical Lennard-Jones type potential:

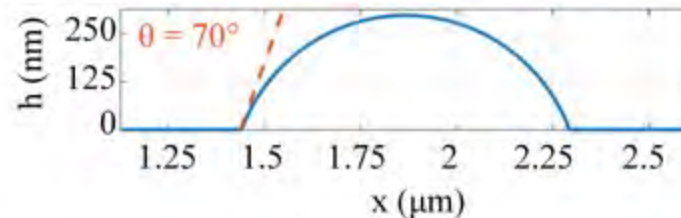
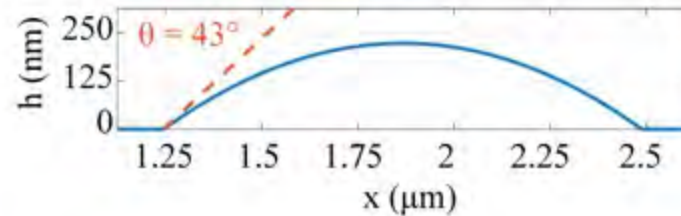
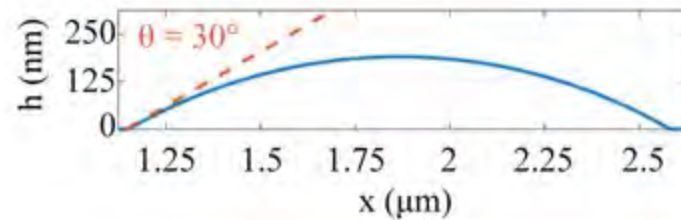
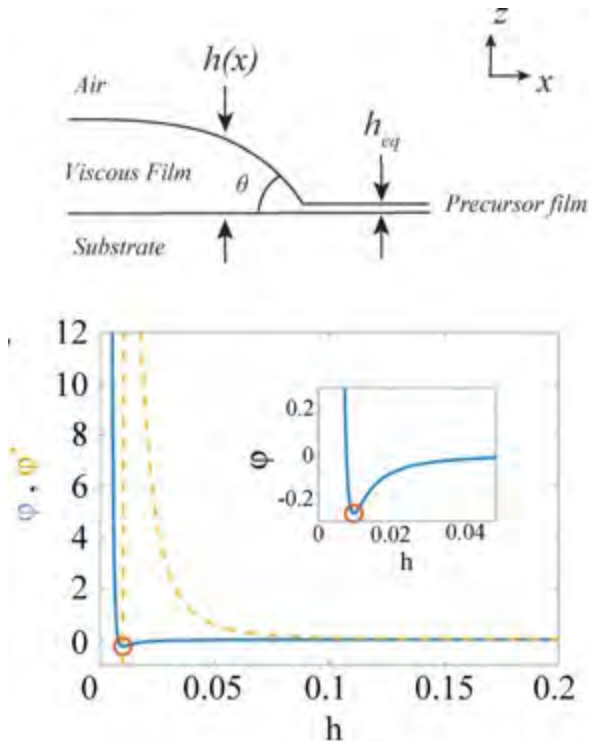
$$\varphi(h) = \frac{B}{h^8} - \frac{A}{12\pi h^2}$$

- where A is the so-called Hamaker constant of the system substrate (1) - film (2) - air (3) and B is the Born coefficient, employed to model respectively the molecular long-range attractive and short-range repulsive forces.
- The combination of a repulsive and an attractive term defines a minimum of the potential for an equilibrium “precursor” film thickness $h_{\text{eq}} = (48\pi B/A)^{1/6}$ obtained by imposing $\varphi'(h_{\text{eq}}) = 0$
- The force derived from the Lennard-Jones potential stems from an imbalance in the interactions between the various constituent molecules. This imbalance is classically embedded in the Hamaker constant, which establishes the influence of constituent materials in long-range interactions, in the presence of multiple bodies according to Lifschitz theory.

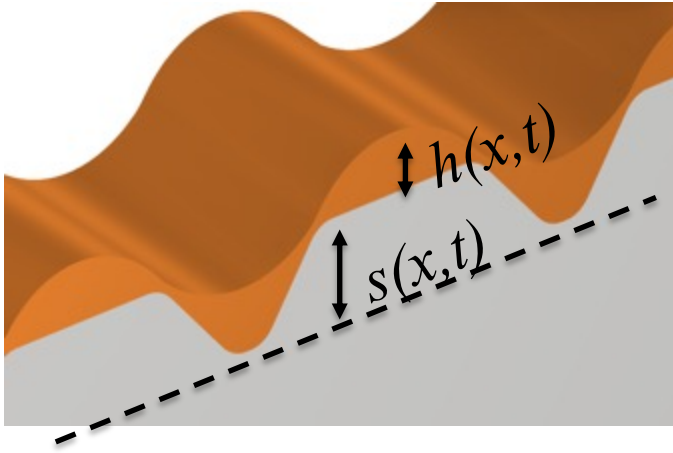
$$\Pi = -\frac{\partial\varphi}{\partial h} = \frac{8B}{h^9} - \frac{A}{6\pi h^3}$$

- A positive Hamaker constant induces destabilizing pressure gradients for films larger than the equilibrium thickness h_{eq} .
- When a region of the film reaches this thickness, the local equilibrium at the interface between the precursor film and the thicker regions defines an apparent contact angle θ

$$1 + \tan^2 \theta = \left(\frac{\varphi(h_{eq})}{\gamma} + 1 \right)^{-2}$$



- The treatment of the textured substrate complicates a bit the mathematics of it.



$$\kappa = -\vec{\nabla} \cdot \mathbf{n}_t$$

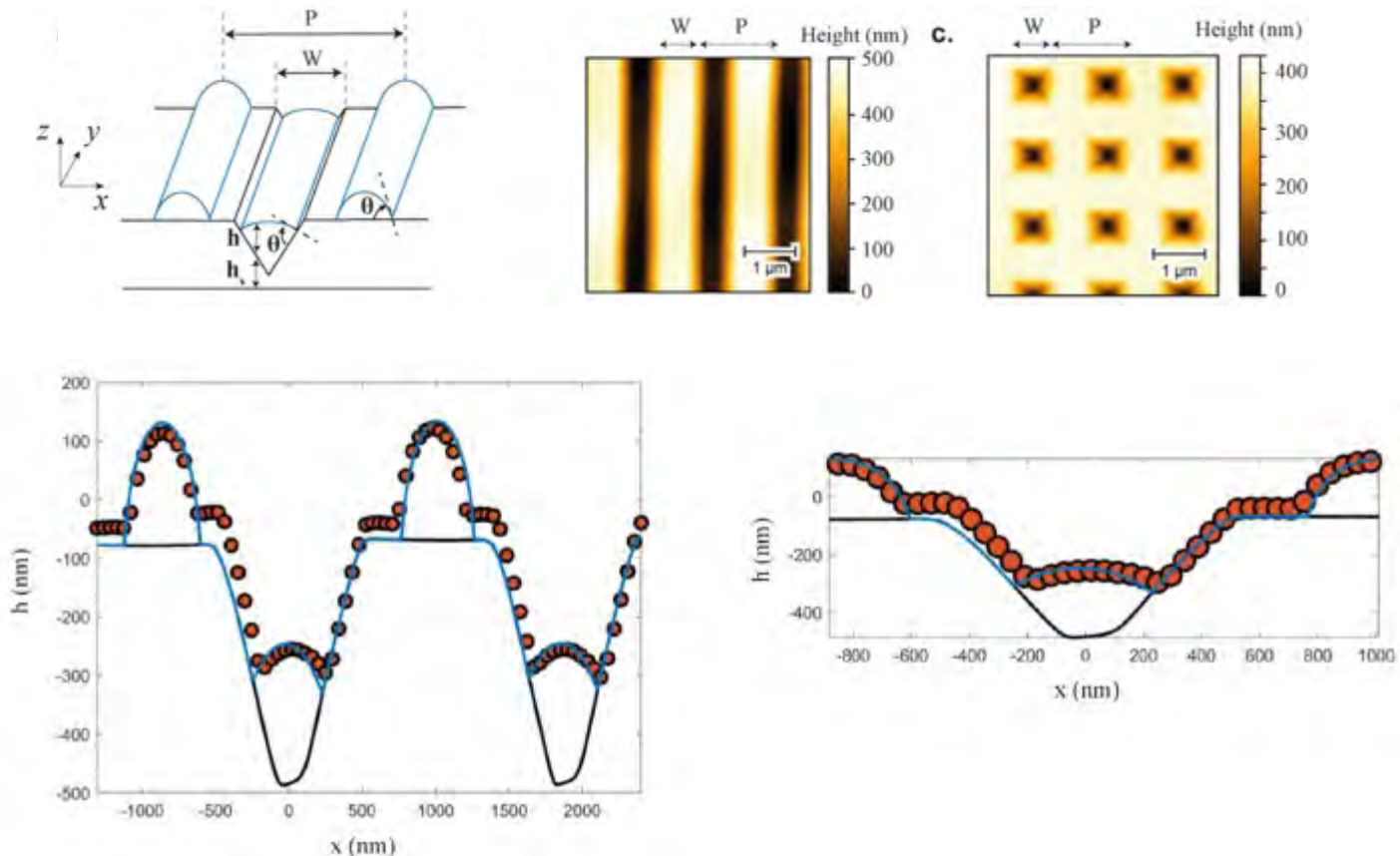
$$\mathbf{n}_t = \frac{1}{\left(1 + \left(\frac{\partial h}{\partial x} + \frac{\partial h_s}{\partial x}\right)^2 + \left(\frac{\partial h}{\partial y} + \frac{\partial h_s}{\partial y}\right)^2\right)^{1/2}} \begin{bmatrix} \left(-\frac{\partial h}{\partial x} - \frac{\partial h_s}{\partial x}\right) \\ \left(-\frac{\partial h}{\partial y} - \frac{\partial h_s}{\partial y}\right) \end{bmatrix}$$

- The definition of the thickness is also important to carefully define. It differs, contrary to the planar configuration, from the total elevation $h + h_s$.

$$h^* = h \cos \left(\arctan \left(\left(\frac{\partial h_s}{\partial x}\right)^2 + \left(\frac{\partial h_s}{\partial y}\right)^2 \right)^{1/2} \right)$$

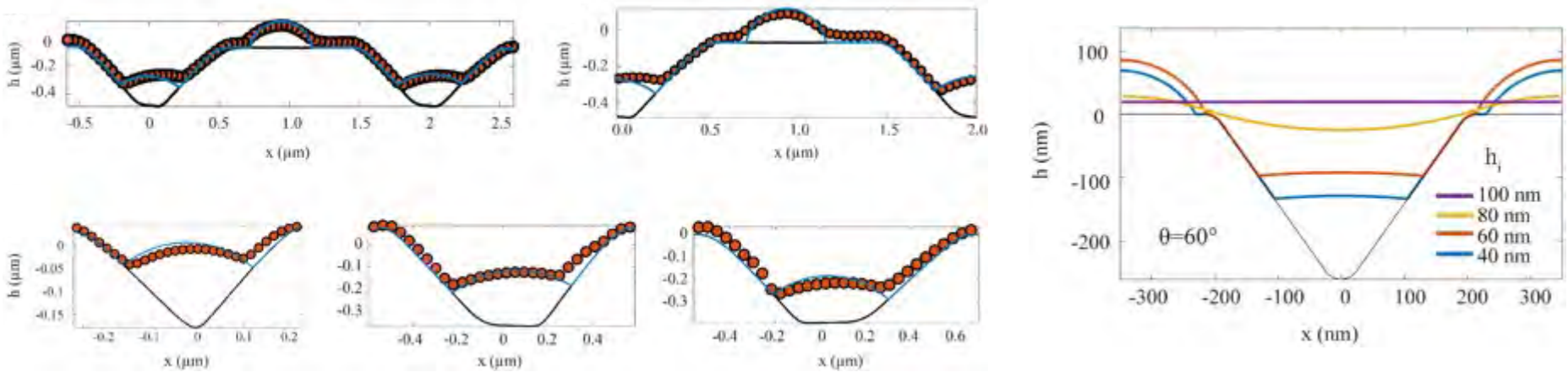
- The simulation used COMSOL physics, a finite-element based approach to model the evolution of a film in 2D and 3D subjected to the following equation:

$$\frac{\partial h}{\partial t} = -\frac{1}{3\mu} \nabla \cdot (h^3 \nabla (\gamma \nabla \kappa - \Pi(h)))$$

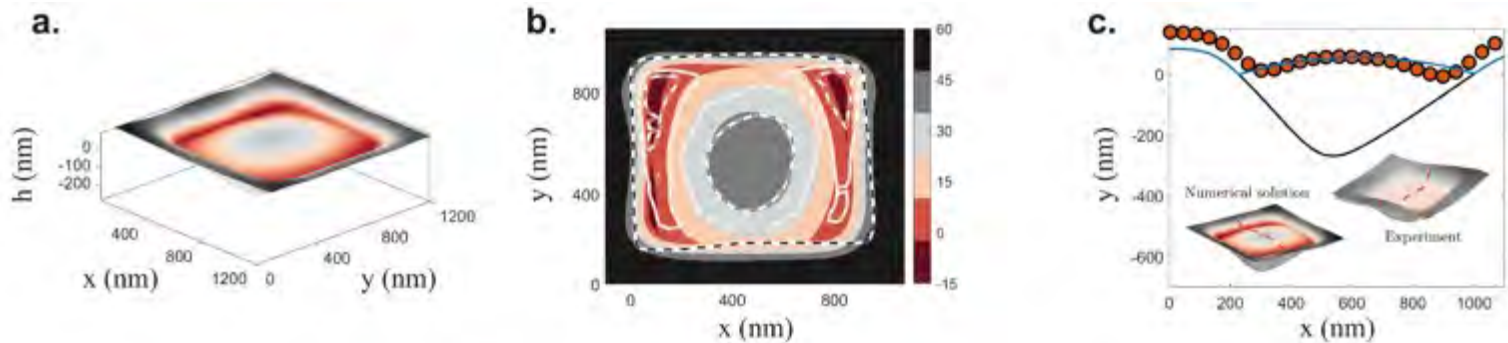


- The dots are experimental values from AFM measurements, and the line represent the model prediction.

- Other simulations for different pattern parameters, as well as the influence of the initial thickness on the shape of the dewetted pattern.

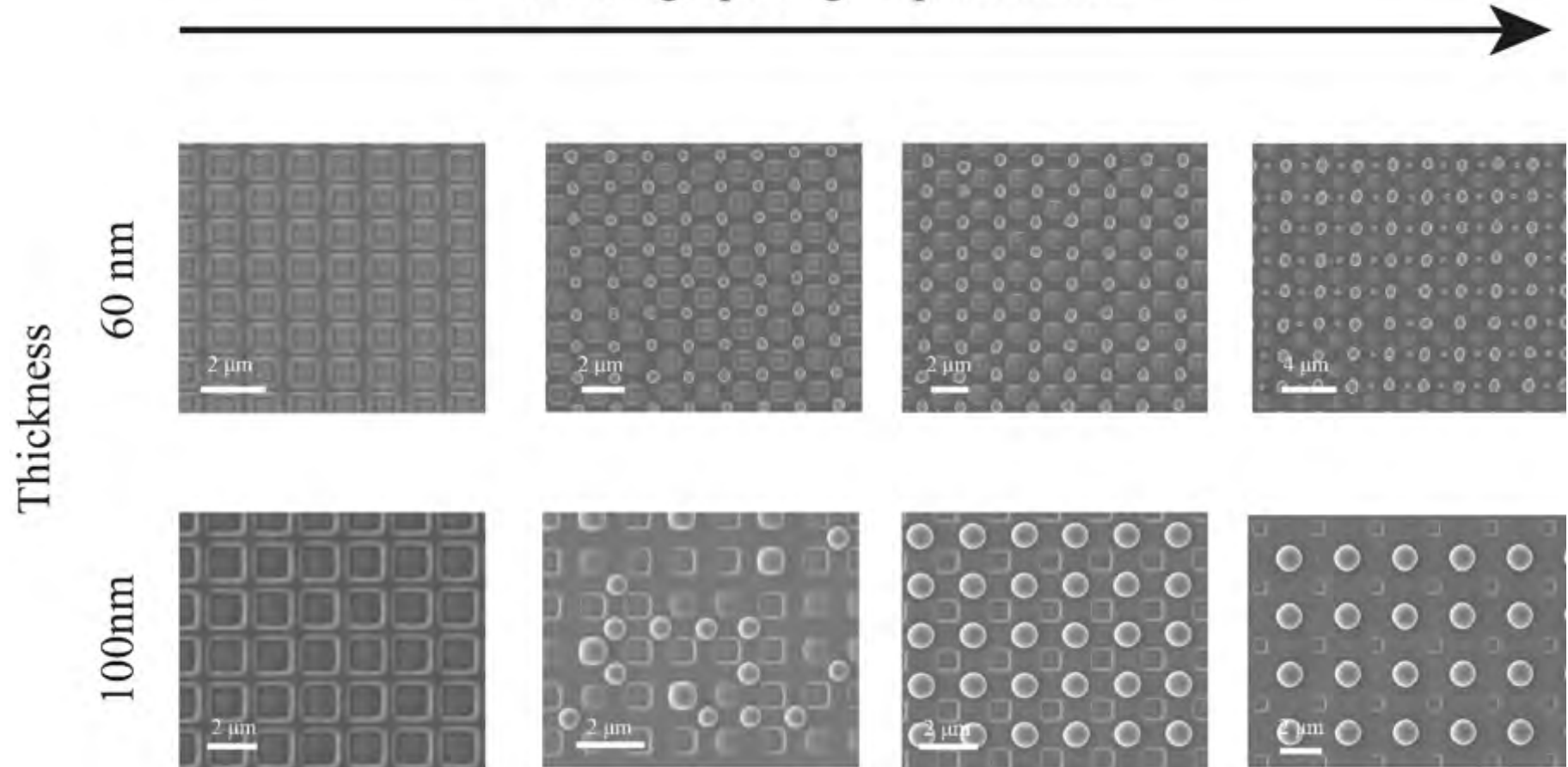


- Although heavier, the simulation also represent well 3D architectures.

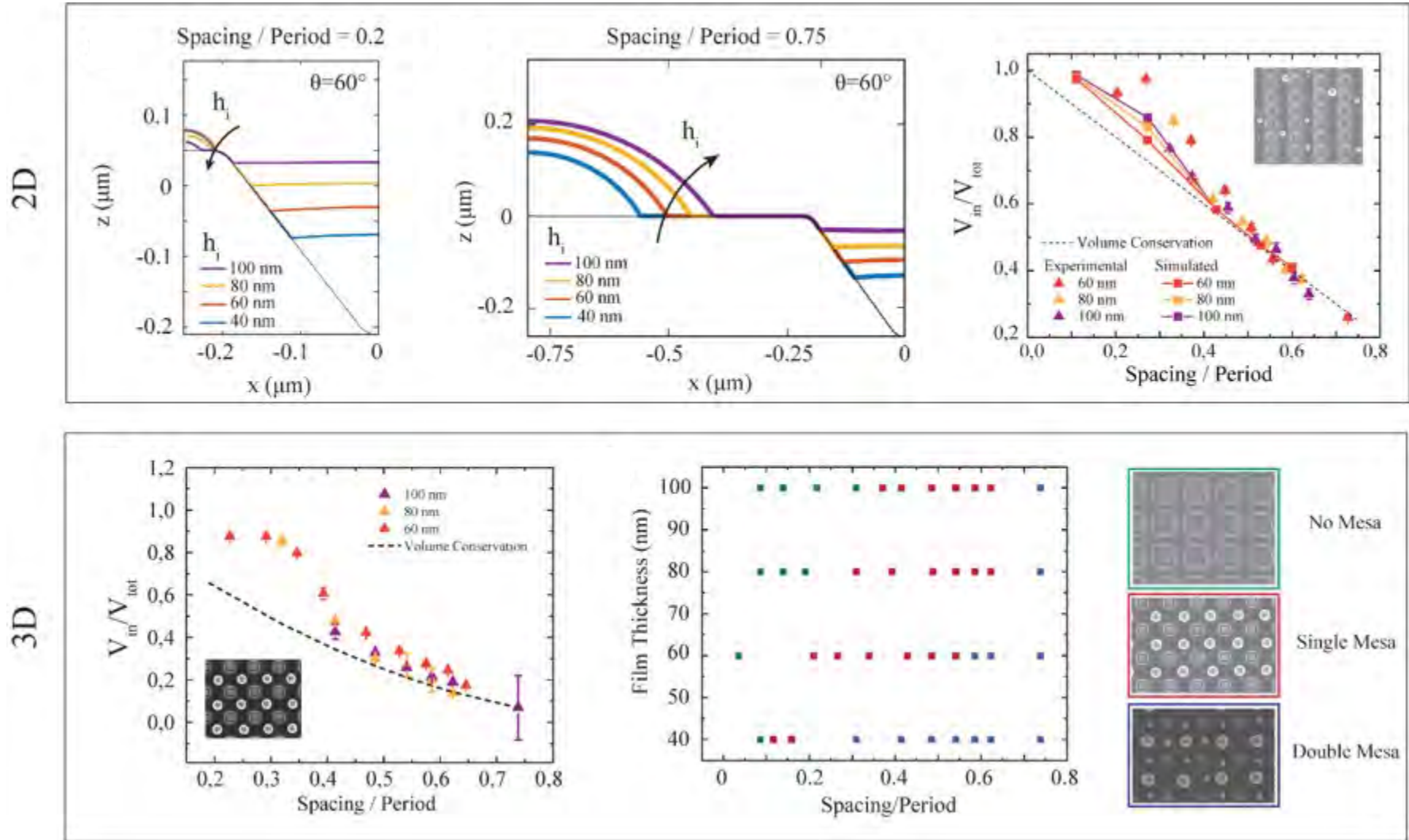


- An important parameter in template dewetting of optical glasses is the effect of period to Mesa ratio in the resulting architectures.

Increasing Spacing-to-period ratio



- Modelling represents well the effect of period to Mesa ratio in templated dewetting architectures.



THANK YOU

Fabien.sorin@epfl.ch

PhD Students

- **Dr. Louis Martin-Monier**
- **Dr. William Esposito**
- **Pierre-Luc Piveteau**
- Stella Laperroussae
- Hritwick Banerjee
- Yan Wei
- Laurène tribolet
- Jinwon Son

Postdoc

- **Dr. DasGupta**
- Dr. Xin Chin
- Dr. Bastien Schyrr

Assistant: Isabel Nzazi

